Fig. 5. Suberoylanilide hydroxamic acid (SAHA) increases the expression of Epstein–Barr virus (EBV)-lytic genes and decreases the expression of EBV-latent genes. EBV-positive T cell lines and natural killer (NK) cell lines were treated with 5 μM SAHA (closed triangles) or control (open circles) and cultured for 24 or 48 h. EBV-encoded gene expression was analyzed using real-time RT-PCR. β2-microglobulin was used as a reference gene for relative quantification, and was assigned an arbitrary value of 1 (10^0). Data are expressed as means ± SEM.
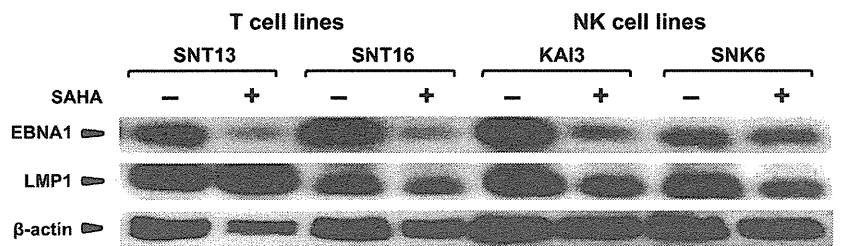

Fig. 6. Suberoylanilide hydroxamic acid (SAHA) decreases the expression of LMP1 and EBNA1 proteins in Epstein–Barr virus (EBV)-positive T and natural killer (NK) cell lines. EBV-positive T and NK cell lines were treated with 5 μM SAHA or DMSO for 48 h. EBNA1 and LMP1 were detected by immunoblotting. β-Actin was used as a loading control.

plays an important role in inhibiting apoptosis.[39] Downregulation of EBNA1 may also be associated with the suppressive effect on the proliferation of EBV-positive T and NK cell lines. Although SAHA downregulated EBV-encoded genes such as EBNA1 and LMP1, the effects of SAHA did not differ between EBV-positive and EBV-negative cell lines. The discrepancy is not clear. The EBV-positive and EBV-negative cell line sets, which were used to verify the presence/absence of EBV in the T and NK cell lines (Fig. 2a), might be inappropriate for the purpose. The EBV-positive cell lines were produced by artificial EBV infections using marker selections.[26,28] The parent cell lines can proliferate vigorously, so they did not need the help of EBV. It is also possible that the change of EBV-associated genes and proteins may be not

the cause, but the result. These questions should be clarified in future studies.

We applied the murine xenograft model to further evaluate the efficacy of SAHA. Using this model, we have shown that SAHA prevented not only tumor growth but also metastasis of EBV-positive NK cell lymphoma. However, the progressive tumor growth was renewed subsequently, suggesting a limitation of single-agent therapy. Synergistic effects of HDAC inhibitors and their combination with mTOR inhibitors have been demonstrated in renal cell and prostate carcinoma cell lines.[40,41] In nasopharyngeal carcinoma, bortezomib and SAHA synergistically induced reactive oxygen species-driven caspase-dependent apoptosis and blocked the replication of EBV.[42] The combination of these agents and SAHA could
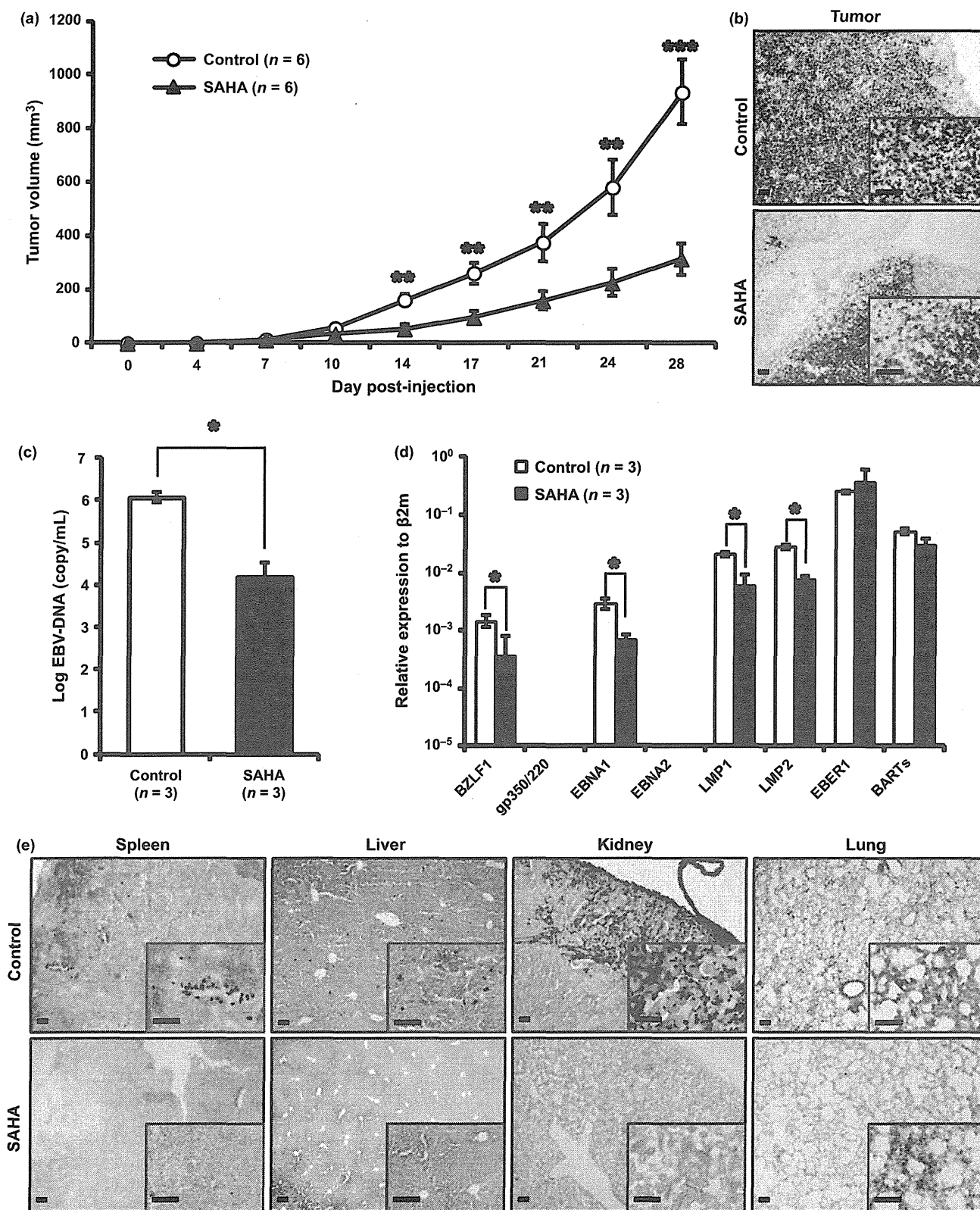
—105—

Fig. 7. Suberoylanilide hydroxamic acid (SAHA) inhibits tumor growth and metastasis of Epstein–Barr virus (EBV)-positive natural killer (NK) cell lymphoma. (a) SNK6 cells (1 × 10⁶ per mouse) were inoculated subcutaneously into NOG mice. Mice were treated with 100 mg/kg SAHA or DMSO (control) daily from days 4 to 28. Tumor sizes were measured twice per week. (b) At 30 days after inoculation, mice were killed, and Epstein–Barr virus-encoded small RNA-positive cells were detected by *in situ* hybridization in tumor tissues of SAHA-treated or control mice (scale bars: 200 μm). (c) At 30 days after inoculation, peripheral blood was collected, and plasma was separated. EBV-DNA was quantified by real-time PCR. (d) At 30 days, EBV-related gene expression in tumor tissues was quantified. β2-Microglobulin was used for relative quantification and assigned an arbitrary value of 1 (10⁰). (e) EBER-positive cells, which meant EBV-positive lymphoma cells, were detected by *in situ* hybridization in organ tissues of SAHA-treated or control mice (scale bars: 200 μm). $*P < 0.05$, $**P < 0.01$, $***P < 0.002$ by Mann–Whitney U-test.

improve the therapy of EBV-associated T and NK cell lymphoma.

In conclusion, SAHA suppressed the proliferation of T and NK cell lines, although no significant difference was observed between EBV-positive and EBV-negative cell lines. SAHA induced apoptosis and/or cell cycle arrest in some T and NK cell lines. Furthermore, SAHA inhibited tumor progression and metastasis in a murine xenograft model. Thus, SAHA had a marked suppressive effect against EBV-associated T and NK cell lymphomas, which was mediated by either induction of apoptosis or cell cycle arrest, and could represent an alternative treatment.

References

1 Cohen JI. Epstein-Barr virus infection. *N Engl J Med* 2000; **343**: 481–92.
2 Williams H, Crawford DH. Epstein-Barr virus: the impact of scientific advances on clinical practice. *Blood* 2006; **107**: 862–9.
3 Suzuki R, Suzumiya J, Yamaguchi M *et al.* Prognostic factors for mature natural killer (NK) cell neoplasms: aggressive NK cell leukemia and extranodal NK cell lymphoma, nasal type. *Ann Oncol* 2010; **21**: 1032–40.
4 Cartron G, Watier H, Golay J, Solal-Celigny P. From the bench to the bedside: ways to improve rituximab efficacy. *Blood* 2004; **104**: 2635–42.
5 Heslop HE. How I treat EBV lymphoproliferation. *Blood* 2009; **114**: 4002–8.
6 Bolden JE, Peart MJ, Johnstone RW. Anticancer activities of histone deacetylase inhibitors. *Nat Rev Drug Discov* 2006; **5**: 769–84.
7 Xu WS, Parmigiani RB, Marks PA. Histone deacetylase inhibitors: molecular mechanisms of action. *Oncogene* 2007; **26**: 5541–52.
8 Iwata S, Saito T, Ito Y *et al.* Antitumor activities of valproic acid on Epstein-Barr virus-associated T and natural killer lymphoma cells. *Cancer Sci* 2012; **103**: 375–81.
9 Richon VM, Zhou X, Rifkind RA, Marks PA. Histone deacetylase inhibitors: development of suberoylanilide hydroxamic acid (SAHA) for the treatment of cancers. *Blood Cells Mol Dis* 2001; **27**: 260–4.
10 Marks PA. Discovery and development of SAHA as an anticancer agent. *Oncogene* 2007; **26**: 1351–6.
11 Stathis A, Hotte SJ, Chen EX *et al.* Phase I study of decitabine in combination with vorinostat in patients with advanced solid tumors and non-Hodgkin's lymphomas. *Clin Cancer Res* 2011; **17**: 1582–90.
12 Munster PN, Thurn KT, Thomas S *et al.* A phase II study of the histone deacetylase inhibitor vorinostat combined with tamoxifen for the treatment of patients with hormone therapy-resistant breast cancer. *Br J Cancer* 2011; **104**: 1828–35.
13 Hui KF, Chiang AK. Suberoylanilide hydroxamic acid induces viral lytic cycle in Epstein-Barr virus-positive epithelial malignancies and mediates enhanced cell death. *Int J Cancer* 2010; **126**: 2479–89.
14 Hui KF, Ho DN, Tsang CM, Middeldorp JM, Tsao GS, Chiang AK. Activation of lytic cycle of Epstein-Barr virus by suberoylanilide hydroxamic acid leads to apoptosis and tumor growth suppression of nasopharyngeal carcinoma. *Int J Cancer* 2012; **131**: 1930–40.
15 Karube K, Tsuzuki S, Yoshida N *et al.* Comprehensive gene expression profiles of NK cell neoplasms identify vorinostat as an effective drug candidate. *Cancer Lett* 2013; **333**: 47–55.
16 Ito M, Hiramatsu H, Kobayashi K *et al.* NOD/SCID/gamma(c)(null) mouse: an excellent recipient mouse model for engraftment of human cells. *Blood* 2002; **100**: 3175–82.
17 Yajima M, Imadome K, Nakagawa A *et al.* A new humanized mouse model of Epstein-Barr virus infection that reproduces persistent infection, lymphoproliferative disorder, and cell-mediated and humoral immune responses. *J Infect Dis* 2008; **198**: 673–82.
18 Shultz LD, Lyons BL, Burzenski LM *et al.* Human lymphoid and myeloid cell development in NOD/LtSz-scid IL2R gamma null mice engrafted with mobilized human hemopoietic stem cells. *J Immunol* 2005; **174**: 6477–89.
19 Sato K, Misawa N, Nie C *et al.* A novel animal model of Epstein-Barr virus-associated hemophagocytic lymphohistiocytosis in humanized mice. *Blood* 2011; **117**: 5663–73.
20 Imadome K, Yajima M, Arai A *et al.* Novel mouse xenograft models reveal a critical role of CD4+ T cells in the proliferation of EBV-infected T and NK cells. *PLoS Pathog* 2011; **7**: e1002326.
21 Zhang Y, Nagata H, Ikeuchi T *et al.* Common cytological and cytogenetic features of Epstein-Barr virus (EBV)-positive natural killer (NK) cells and cell lines derived from patients with nasal T/NK-cell lymphomas, chronic

active EBV infection and hydroa vacciniforme-like eruptions. *Br J Haematol* 2003; **121**: 805–14.
22 Kaplan J, Tilton J, Peterson WD. Identification of T cell lymphoma tumor antigens on human T cell lines. *Am J Hematol* 1976; **1**: 219–23.
23 Tsuge I, Morishima T, Morita M, Kimura H, Kuzushima K, Matsuoka H. Characterization of Epstein-Barr virus (EBV)-infected natural killer (NK) cell proliferation in patients with severe mosquito allergy; establishment of an IL-2-dependent NK-like cell line. *Clin Exp Immunol* 1999; **115**: 385–92.
24 Yagita M, Huang CL, Umehara H *et al.* A novel natural killer cell line (KHYG-1) from a patient with aggressive natural killer cell leukemia carrying a p53 point mutation. *Leukemia* 2000; **14**: 922–30.
25 Miyoshi I, Kubonishi I, Yoshimoto S *et al.* Type C virus particles in a cord T-cell line derived by co-cultivating normal human cord leukocytes and human leukaemic T cells. *Nature* 1981; **294**: 770–1.
26 Fujiwara S, Ono Y. Isolation of Epstein-Barr virus-infected clones of the human T-cell line MT-2: use of recombinant viruses with a positive selection marker. *J Virol* 1995; **69**: 3900–3.
27 Robertson MJ, Cochran KJ, Cameron C, Le JM, Tantravahi R, Ritz J. Characterization of a cell line, NKL, derived from an aggressive human natural killer cell leukemia. *Exp Hematol* 1996; **24**: 406–15.
28 Isobe Y, Sugimoto K, Matsuura I, Takada K, Oshimi K. Epstein-Barr virus renders the infected natural killer cell line, NKL, resistant to doxorubicin-induced apoptosis. *Br J Cancer* 2008; **99**: 1816–22.
29 Iwata S, Yano S, Ito Y *et al.* Bortezomib induces apoptosis in T lymphoma cells and natural killer lymphoma cells independent of Epstein-Barr virus infection. *Int J Cancer* 2011; **129**: 2263–73.
30 Wang D, Liebowitz D, Wang F *et al.* Epstein-Barr virus latent infection membrane protein alters the human B-lymphocyte phenotype: deletion of the amino terminus abolishes activity. *J Virol* 1988; **62**: 4173–84.
31 Daikoku T, Kudoh A, Fujita M, Sugaya Y, Isomura H, Tsurumi T. In vivo dynamics of EBNA1-oriP interaction during latent and lytic replication of Epstein-Barr virus. *J Biol Chem* 2004; **279**: 54817–25.
32 Iwata S, Wada K, Tobita S *et al.* Quantitative analysis of Epstein-Barr virus (EBV)-related gene expression in patients with chronic active EBV infection. *J Gen Virol* 2010; **91**: 42–50.
33 Kubota N, Wada K, Ito Y *et al.* One-step multiplex real-time PCR assay to analyse the latency patterns of Epstein-Barr virus infection. *J Virol Methods* 2008; **147**: 26–36.
34 Patel K, Whelan PJ, Prescott S *et al.* The use of real-time reverse transcription-PCR for prostate-specific antigen mRNA to discriminate between blood samples from healthy volunteers and from patients with metastatic prostate cancer. *Clin Cancer Res* 2004; **10**: 7511–9.
35 Murata T, Iwata S, Siddiquey MN *et al.* Heat shock protein 90 inhibitors repress latent membrane protein 1 (LMP1) expression and proliferation of Epstein-Barr virus-positive natural killer cell lymphoma. *PLoS ONE* 2013; **8**: e63566.
36 Kimura H, Morita M, Yabuta Y *et al.* Quantitative analysis of Epstein-Barr virus load by using a real-time PCR assay. *J Clin Microbiol* 1999; **37**: 132–6.
37 Longnecker RM, Kieff E, Cohen JI. Epstein-Barr virus. In: Knipe DM, Howley PM, eds. *Fields Virology*, 6th edn. Philadelphia: Wolters kluwer/Lippincott Williams & Wilkins, 2013; 1898–959.
38 Damania B. Oncogenic gamma-herpesviruses: comparison of viral proteins involved in tumorigenesis. *Nat Rev Microbiol* 2004; **2**: 656–68.
39 Saridakis V, Sheng Y, Sarkari F *et al.* Structure of the p53 binding domain of HAUSP/USP7 bound to Epstein-Barr nuclear antigen 1 implications for EBV-mediated immortalization. *Mol Cell* 2005; **18**: 25–36.
40 Mahalingam D, Medina EC, Esquivel JA *et al.* Vorinostat enhances the activity of temsirolimus in renal cell carcinoma through suppression of survivin levels. *Clin Cancer Res* 2010; **16**: 141–53.

41 Thelen P, Krahn L, Bremmer F, Strauss A, Brehm R, Loertzer H. Synergistic effects of histone deacetylase inhibitor in combination with mTOR inhibitor in the treatment of prostate carcinoma. *Int J Mol Med* 2013; **31**: 339–46.

42 Hui KF, Lam BH, Ho DN, Tsao SW, Chiang AK. Bortezomib and SAHA synergistically induce ROS-driven caspase-dependent apoptosis of nasopharyngeal carcinoma and block replication of Epstein-Barr virus. *Mol Cancer Ther* 2013; **12**: 747–58.

Supporting Information

Additional supporting information may be found in the online version of this article:

Fig. S1. SNK6 is less dependent of human interleukin-2 (IL-2) compared with other Epstein–Barr virus (EBV)-positive T and natural killer (NK) cell lines.

Table S1. Engraftment of cell lines into NOG mice.

CD137 Expression Is Induced by Epstein-Barr Virus Infection through LMP1 in T or NK Cells and Mediates Survival Promoting Signals

Mayumi Yoshimori[1,2], Ken-Ichi Imadome[3], Honami Komatsu[1,2], Ludan Wang[1], Yasunori Saitoh[4], Shoji Yamaoka[4], Tetsuya Fukuda[1], Morito Kurata[5], Takatoshi Koyama[2], Norio Shimizu[6], Shigeyoshi Fujiwara[3], Osamu Miura[1], Ayako Arai[1]*

1 Department of Hematology, Graduate School of Medical and Dental Sciences, Tokyo Medical and Dental University, Tokyo, Japan, 2 Department of Laboratory Molecular Genetics of Hematology, Graduate School of Health Care Sciences, Tokyo Medical and Dental University, Tokyo, Japan, 3 Department of Infectious Diseases, National Research Institute for Child Health and Development, Tokyo, Japan, 4 Department of Molecular Virology, Graduate School of Medical and Dental Sciences, Tokyo Medical and Dental University, Tokyo, Japan, 5 Department of Comprehensive Pathology, Graduate School of Medical and Dental Sciences, Tokyo Medical and Dental University, Tokyo, Japan, 6 Department of Virology, Division of Medical Science, Medical Research Institute, Tokyo Medical and Dental University, Tokyo, Japan

Abstract

To clarify the mechanism for development of Epstein-Barr virus (EBV)-positive T- or NK-cell neoplasms, we focused on the costimulatory receptor CD137. We detected high expression of CD137 gene and its protein on EBV-positive T- or NK-cell lines as compared with EBV-negative cell lines. EBV-positive cells from EBV-positive T- or NK-cell lymphoproliferative disorders (EBV-T/NK-LPDs) patients also had significantly higher CD137 gene expression than control cells from healthy donors. In the presence of IL-2, whose concentration in the serum of EBV-T/NK-LPDs was higher than that of healthy donors, CD137 protein expression was upregulated in the patients' cells whereas not in control cells from healthy donors. In vitro EBV infection of MOLT4 cells resulted in induction of endogenous CD137 expression. Transient expression of LMP1, which was enhanced by IL-2 in EBV-T/NK-LPDs cells, induced endogenous CD137 gene expression in T and NK-cell lines. In order to examine in vivo CD137 expression, we used EBV-T/NK-LPDs xenograft models generated by intravenous injection of patients' cells. We identified EBV-positive and CD8-positive T cells, as well as CD137 ligand-positive cells, in their tissue lesions. In addition, we detected CD137 expression on the EBV infected cells from the lesions of the models by immune-fluorescent staining. Finally, CD137 stimulation suppressed etoposide-induced cell death not only in the EBV-positive T- or NK-cell lines, but also in the patients' cells. These results indicate that upregulation of CD137 expression through LMP1 by EBV promotes cell survival in T or NK cells leading to development of EBV-positive T/NK-cell neoplasms.

Introduction

Epstein-Barr virus (EBV) infection can be found in lymphoid malignancies not only of B-cell lineage, but also of T- or NK-cell lineages. These EBV-positive T or NK-cell neoplasms, such as extranodal NK/T-cell lymphoma nasal type (ENKL), aggressive NK-cell leukemia (ANKL), and EBV-positive T- or NK- cell lymphoproliferative diseases (EBV-T/NK-LPDs), are relatively rare but lethal disorders classified as peripheral T/NK-cell lymphomas according to the WHO classification of tumors of hematopoietic and lymphoid malignancies. ENKL is a rapidly progressive lymphoma characterized by extranodal lesions with vascular damage and severe necrosis accompanied by infiltration of neoplastic NK or cytotoxic T cells [1]. ANKL is a markedly aggressive leukemia with neoplastic proliferation of NK cells [2]. EBV-T/NK-LPDs is a fatal disorder presenting sustained infectious mononucleosis-like symptoms, hypersensitivity to mos-

quito bites, or hydroa vacciniforme-like eruption accompanied by clonal proliferation of EBV-infected cells [3,4]. Because most reported cases were children or young adults, and were mainly of the T-cell-infected type, the disorders were designated "EBV-positive T-cell lymphoproliferative diseases of childhood" in the WHO classification, although adult and NK-cell types have been reported [4–6]. The common clinical properties of EBV-T/NK-neoplasms are the presence of severe inflammation, resistance to chemotherapy, and a marked geographic bias for East Asia and Latin America, suggesting a genetic context for disease development [4]. Since these EBV-T/NK-neoplasms overlap [4], common mechanisms are thought to exist in the background and contribute to disease development.

It is well known that EBV infects B cells and makes the infected cells immortal resulting in B-cell lymphomas. Similarly it is suspected that EBV may also cause T- or NK-cell neoplasms. However, why and how EBV latently infects T or NK cells,

whether or not EBV directly causes these malignancies, and the mechanism of action responsible for the disease development remain to be clarified. Although new chemotherapy and stem cell transplantation have achieved good results for EBV-T/NK neoplasms recently [7–9], prognosis of the diseases is still poor. The mechanisms for development of the disease need to be determined to establish an optimal treatment.

To clarify the molecular mechanism underlying the development of EBV-T/NK-neoplasms, we focused on the costimulatory receptor CD137. CD137, also known as 4-1BB, is a member of the tumor necrosis factor (TNF) receptor superfamily, and expressed on the surface of activated T and NK cells [10]. In association with TCR stimulation, it plays a pivotal role in proliferation, survival, and differentiation of these cells as a costimulatory molecule [11]. Recently, it was reported that CD137 is expressed on tumor cells from adult T-cell leukemia/lymphoma (ATLL) and from T-cell lymphomas [12,13]. Here we found CD137 expression on EBV-positive cells in EBV-T/NK-neoplasms and investigated its role for the lymphomagenesis using established cell lines as well as cells from EBV-T/NK-LPDs patients.

Results

CD137 expression in EBV-T/NK-cell lines

Six EBV-positive T- and NK-cell lines, SNT8, SNT15, SNT16, SNK1, SNK6, and SNK10 had been established from primary lesions of ENKL patients (SNT8 and SNK6) and PB of EBV-T/NK-LPDs patients (SNT15, SNT16, SNK1, and SNK10) [14]. We investigated *CD137* mRNA expression in the cell lines by RT-PCR. *CD137* mRNA was expressed in all of them, whereas EBV-negative T-cell lines (Jurkat, MOLT4, and HPB-ALL) and NK-cell line (KHYG1) were negative for the expression (Figure 1A). The mRNA was detected but weak in an EBV-negative NK-cell line, MTA, and in EBV-negative B-cell lines, BJAB, Ramos, and MD901. We also investigated 3 EBV-positive B cell lines, Raji, a lymphoblastoid cell line (LCL), and HS-sultan. The expression was detected in Raji. The expression was weak in LCL, and negative in HS-Sultan. We next investigated CD137 protein expression on the cell surface. Figure 1B shows that CD137 protein was expressed on the cell surface of all EBV-positive T- or NK-cells. In contrast, EBV-negative T-, NK-, and B-cell lines were negative for CD137 expression. On the basis of these results, we concluded that CD137 expression was induced at the mRNA and protein levels in EBV-T/NK cell lines. The expression was detected in 2 of 3 examined EBV-positive B cell lines, Raji and LCL, whereas negative in HS-Sultan. The expression in EBV-positive B cells was insignificant in comparison with EBV-positive T or NK cells. We were unable to detect CD137L expression on the surface these EBV-positive T- or NK-cells lines. The expression was negative on them (Figure S1).

EBV induces CD137 expression in T and NK cells

To clarify whether EBV could directly induce CD137 expression, we performed *in vitro* EBV infection of an EBV-negative cell line MOLT4. EBV DNA copy number of EBV-infected MOTL4 cells was 8.8×10^5 copies/µgDNA. EBV infection was verified by the presence of EBV nuclear antigen (EBNA) 1 protein expression (Figure 2A). Most cells were positive for EBNA1. The infection was also confirmed by the presence of the viral mRNA, *LMP1* and *EBNA1*, and the absence of *EBNA2* by RT-PCR (Figure 2B). This expression pattern was classified as latency type 2. *CD137* mRNA was also expressed in EBV-infected MOTL4 cells (Figure 2B and 2C). In addition, Figure 2D showed that CD137 protein expression was detected on EBV-infected

MOLT4 cells. We therefore concluded that EBV infection induced mRNA and surface protein expression of CD137 in MOLT4 cells.

CD137 expression in cells from EBV-T/NK-LPDs patients

The above results were validated using EBV-T/NK cells derived from patients. In EBV-T/NK-LPDs, EBV infection could be detected in a particular fraction of PBMCs and isolated at high purity using antibody-conjugated magnetic beads as described in "Materials and Methods". Seventeen patients (aged 8–72 years; 7 males, 10 females; 10 T- and 7 NK-cell types; CD4 type n = 4, CD8 type n = 5, γδ type n = 1, and CD56 type n = 7) were diagnosed with EBV-T/NK-LPDs according to the criteria as described in "Materials and Methods". We determined the EBV-positive fraction of the lymphocytes in the PB at the diagnosis. The phenotype of the infected cells and EBV DNA load of them were presented in Table 1. EBV DNA was negative or relatively low in CD19-positive cell which EBV can infect (Table 1).

To examine CD137 expression in the EBV-positive fraction, the fractions were isolated by the magnetic beads and obtained for *CD137* mRNA detection in 10 patients. Figure 3A shows the *CD137* mRNA levels in the freshly isolated cells of EBV-positive cell fraction in PBMCs of each patient. *CD137* mRNA levels in CD4-, CD8-, and CD56-positive cell fractions of 5 healthy donors' PBMCs were also demonstrated. The mRNA levels in the patients' cells were significantly higher than those in the cells of healthy donors. Next we examined the expression of CD137 protein by flow cytometry. It showed low expression in freshly isolated PBMCs from both patients and 5 healthy donors (data not shown). However, after culture with IL-2 for 3 days, the expression was increased on the surface of PBMCs from 15 patients but still low on the cells isolated from 5 healthy donors (Figure 3B). The average of CD137 protein levels of EBV-T/NK-LPDs patients was significantly higher than that of healthy donors (Figure 3C). Two-color flow cytometry using antibodies to CD137 and to surface proteins expressed on EBV-positive cells could be performed in 7 patients, and a double-staining pattern was observed in them, whereas fractions from a healthy donor barely expressed the CD137 protein. (Figure S2).

EBV LMP1 induces CD137 expression in T and NK cells through LMP1 induced by IL-2

We investigated the mechanism of enhanced-CD137 expression by IL-2. First we performed luciferase reporter assay with a plasmid containing the *CD137* gene promoter. As shown in Figure 2A, EBV-infected MOLT4 cells were shown to express EBV-encoded proteins including LMP1, and EBNA1, considered to be latency type 2. So, MOLT4 cells were cotransfected with expression plasmids capable of expressing either of EBV-encoded proteins, LMP1, LMP2A, LMP2B or EBNA1. As shown in Figure 4A, LMP1 induced significant upregulation of *CD137* promoter activity, whereas the other molecules did not. Furthermore, in a transient expression assay with these viral proteins in MOLT4 cells, transcription of endogenous *CD137* mRNA was detected only in the LMP1-transfected cells (Figure 4B). These results indicated that, among the EBV proteins, LMP1 transactivated *CD137* expression in T and NK cells. Next we examined whether LMP1 expression was enhanced by IL-2 and might contribute to upregulation of CD137 expression in patients' cells. We isolated PBMCs from EBV-T/NK-LPDs patient (CD4-1) and cultured them with or without IL-2. As shown in Figure 4C, semi-quantitative RT-PCR demonstrated that *LMP1* mRNA was increased in IL-2-treated PBMCs. *CD137* mRNA was also increased in the IL-2-treated cells (Figure 4D). To confirm the
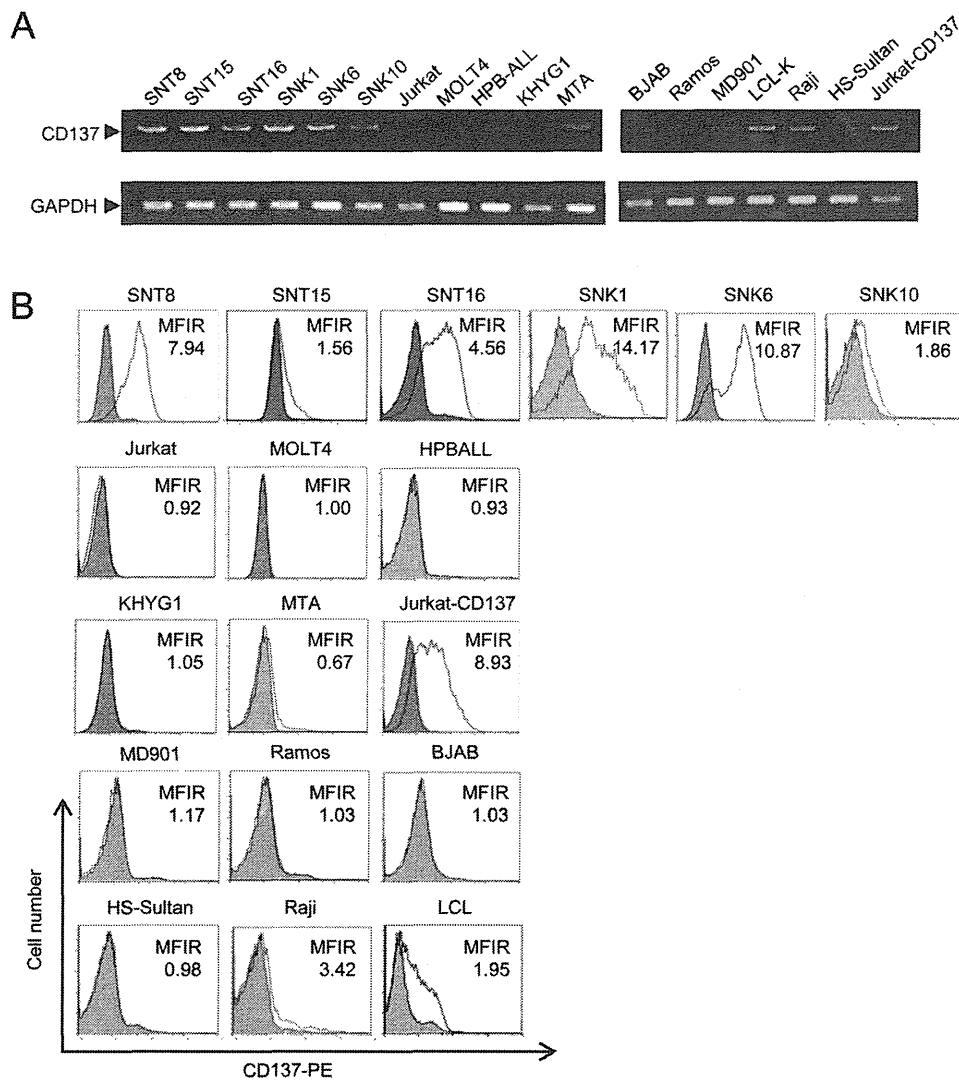
—110—

Figure 1. CD137 expression in Epstein-Barr virus (EBV)-positive T- or NK-cell lines. (A) Transcripts of *CD137* (the upper panel) and *GAPDH* (the lower panel) in EBV- positive T- or NK-cell lines were examined by RT-PCR. EBV negative T-, NK, B-cell lines, and EBV-positive B-cell lines were also obtained for the examination. (B) Surface expression of CD137 was examined by flow cytometry using an antibody to CD137 (open histogram) or isotype-matched control immunoglobulin (gray, shaded histogram). The mean fluorescent intensity of CD137 was normalized by that of isotype-matched control and expressed as mean fluorescence intensity rate (MFIR). Each experiment was independently performed more than 3 times and their average data are presented.
doi:10.1371/journal.pone.0112564.g001

in vivo contribution of IL-2 for CD137 expression, we examined the serum concentration of IL-2 in 7 EBV-T/NK-LPDs patients and 5 healthy donors. The concentration in the patients was 0.9-2.4 U/mL in 6 of 7 patients, whereas it was undetectable in 4 of 5 healthy donors (Table 2). These results suggested that CD137 expression was enhanced in the presence of IL-2 most likely through enhanced-expression of LMP1 in EBV-T/NK-LPDs patient cells.

CD137 was detected in EBV-positive cells infiltrating in the tissue lesion of EBV-T/NK-LPDs xenograft model

Next, we examined the CD137 expression on the EBV-positive cells infiltrating into the tissue of EBV-T/NK-LPDs. Since we could not perform the examination for human specimen due to difficulty of obtaining the samples, we used the xenograft models generated by intravenous injection of PBMCs from CD8-3 patient [15]. The injected cells were 2×10^6 in number for each mouse and

include CD8-positive EBV-infected cells with clonally proliferation from CD8-3 patient. EBV DNA load of the infected cells were more than 1.0×10^4 copies/µgDNA. After engraftment, which was defined as detection of EBV DNA in the PB of the model, we performed autopsy. Nine mice were examined and the representative data were shown. As shown in Figure 5A–D, infiltration of EBV-positive and CD8-positive cells into the periportal regions in the liver was detected. 79.2% (396/500) of the infiltrating cells were EBER-positive, and 77.4% (387/500) of the cells were CD8-positive. These results indicated that most infiltrating cells were both positive for CD8 and EBER. Although CD137L-positive cells were also detected in the lesion, the number was markedly smaller than that of EBV-positive cells (Figure 5D). In order to determine CD137 expression on EBV-infected cells, we performed immune-fluorescent staining for the infiltrating cells in the lesions. As shown in Figure 5E, EBNA1-positive and CD137-positive cells were detected in the cells isolated from the lesions. LMP1 expression
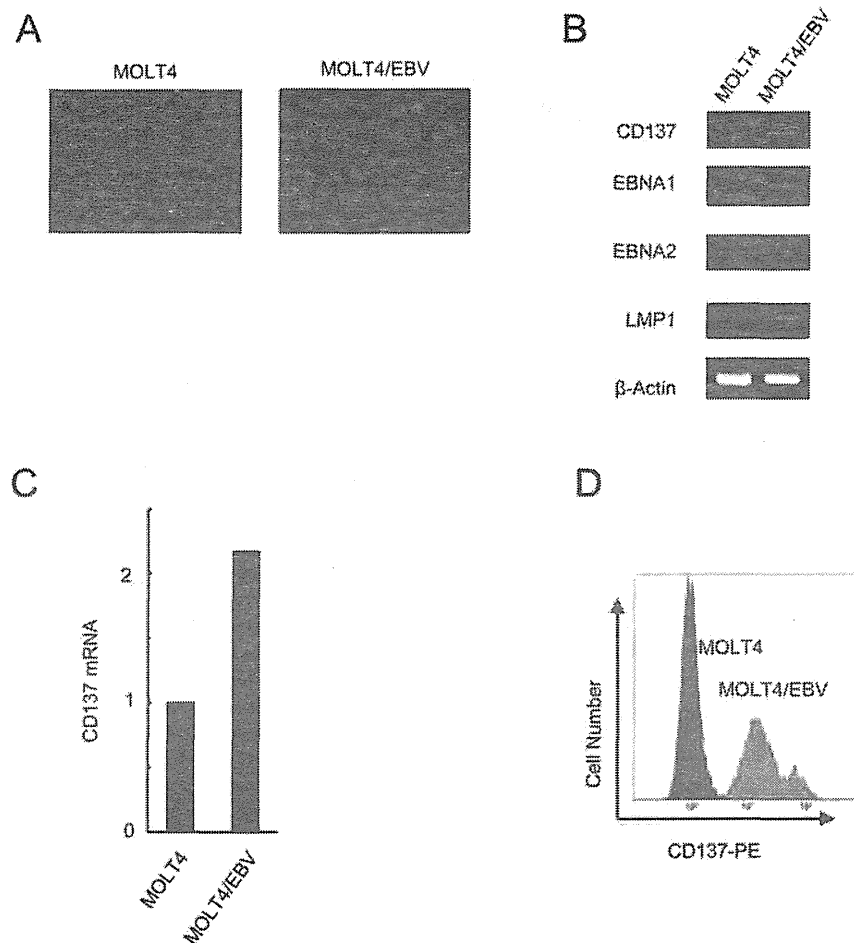
3

—111—

Figure 2. EBV induces CD137 expression in T cells. *In vitro* EBV infection assay performed in MOLT4 cells. (A) EBNA1 protein expression was examined by immune fluorescence staining, 48 hours after the infection, the time when CD137 expression was examined. (B) Expression of the *CD137* gene was examined by RT-PCR. The infection was confirmed by detecting mRNAs of the viral proteins, EBNA1 and LMP1. (C) Transcripts of *CD137* and *GAPDH* were quantified by real time RT-PCR. Relative copy number was obtained by normalizing the *CD137* transcripts to those of those of *GAPDH*. (D) Surface expression of CD137 of MOLT4 cells and EBV-infected MOLT4 cells was examined by flow cytometry.
doi:10.1371/journal.pone.0112564.g002

was confirmed in them (Figure S3). These results indicated that the infiltrating EBV-positive cells were both CD8- and CD137-positive.

Stimulation of CD137 decreases etoposide–induced cell death of EBV-T/NK cells

To explore the contribution of CD137 expression on EBV-T/NK cells to the development of EBV-T/NK-LPDs, we investigated the effects of CD137 on the survival. CHO-CD137L cells with stable expression of human CD137L on their surface were prepared for CD137 stimulation of EBV-T/NK cells (Figure 6A).

First we performed the assay for EBV-positive T- and NK-cell lines. We cocultured the cells with PKH-26-stained CHO cells in the presence of IL-2 with or without etoposide. Jurkat cells were used as a negative control. After the time indicated, we removed the cells and determined the number of living cells by detecting PKH-26 and DiOC6. PKH-26-negative cells were EBV-positive T/NK-cells and Jurkat cells. DiOC6-positive cells were living cells. In the presence of etoposide, the relative number of living EBV-positive T/NK-cells cultured with CHO-CD137L cells was significantly higher than that cultured with control CHO cells (Figure 6B). In contrast, T-cell line Jurkat cells, on which CD137

was not detected (Figure 1B), did not show a difference when cocultured with the 2 types of CHO cells (Figure 6B). In the absence of etoposide, CD137L had no significant effect on the viability of these cells (Figure 6B).

Next we performed the same assay for the primary cells from EBV-T/NK-LPDs patients. We cocultured PBMCs from 2 patients, CD4-2 and CD56-7 with PKH-26-stained CHO cells in the presence of IL-2 with or without etoposide. In the presence of etoposide, the relative number of living cells from EBV-T/NK-LPDs patients cultured with CHO-CD137L cells was significantly higher than that cultured with control CHO cells (Figure 6C). In contrast, cells form a healthy donor did not show a difference when cocultured with the 2 types of CHO cells (Figure 6C). These findings indicated that stimulation of CD137 significantly suppressed etoposide-induced cell death of the EBV-T/NK-LPDs cells.

Discussion

CD137 is expressed following activation of T or NK cells and mediates molecular signals for proliferation, survival, and cytokine production by acting as a costimulatory molecule of the CD3-TCR complex [11,16,17]. However, few data for its roles in

—112—

Table 1. Clinical information of the patients' samples subjected to the assay.

Case	Gender	Age	Infected cell	Clinical findings	EBV-DNA (copies/µgDNA) of PB (whole blood)	EBV-DNA (copies/µgDNA) of the EBV-infected cells fraction in PB	EBV-DNA (copies/µgDNA) of CD19-positive cells fraction in PB
CD4-1	M	45	CD4	sCAEBV	3.1×10^2	4.4×10^4 (CD4)	4.4×10^2
CD4-2	F	25	CD4	HMB	7.0×10^4	2.2×10^5 (CD4)	N.D.
CD4-3	F	62	CD4	sCAEBV	3.2×10^4	4.6×10^5 (CD4)	N.D.
CD4-4	F	72	CD4	sCAEBV	9.4×10^4	6.4×10^5 (CD4)	N.D.
CD8-1	F	38	CD8	sCAEBV	1.4×10^5	3.9×10^5 (CD8)	N.D.
CD8-2	F	21	CD8	sCAEBV	1.9×10^3	4.2×10^4 (CD8)	N.D.
CD8-3	F	64	CD8	sCAEBV	2.6×10^5	1.2×10^6 (CD8)	4.6×10^5
CD8-4	M	28	CD8	sCAEBV	1.9×10^3	4.1×10^5 (CD8)	2.0×10^4
CD8-5	M	13	CD8	sCAEBV	2.1×10^3	6.4×10^4 (CD8)	N.D.
$\gamma\delta$	M	9	$\gamma\delta$	HV	8.0×10^3	2.6×10^4 ($\gamma\delta$)	N.D.
CD56-1	F	18	CD56	sCAEBV	2.5×10^2	5.0×10^4 (CD56)	N.D.
CD56-2	F	13	CD56	HMB	5.2×10^4	1.6×10^6 (CD56)	7.5×10^4
CD56-3	F	23	CD56	sCAEBV	1.0×10^4	1.1×10^5 (CD56)	N.D.
CD56-4	F	48	CD56	sCAEBV	8.6×10^4	1.6×10^5 (CD56)	N.D.
CD56-5	M	9	CD56	sCAEBV	1.1×10^4	5.2×10^5 (CD56)	N.D.
CD56-6	M	8	CD56	sCAEBV	5.1×10^2	3.5×10^4 (CD56)	N.D.
CD56-7	M	24	CD56	sCAEBV	2.3×10^3	2.1×10^4 (CD56)	N.D.

M: Male, F: Female.
EBV: Epstein-Barr virus, PB: peripheral blood.
sCAEBV: systemic chronic active Epstein-Barr virus infection, HMB: hypersensitivity to mosquito bites (HMB), HV: hydroa vacciniforme-like eruption.
*The clonality was detected by Southern blotting for EBV terminal repeat.
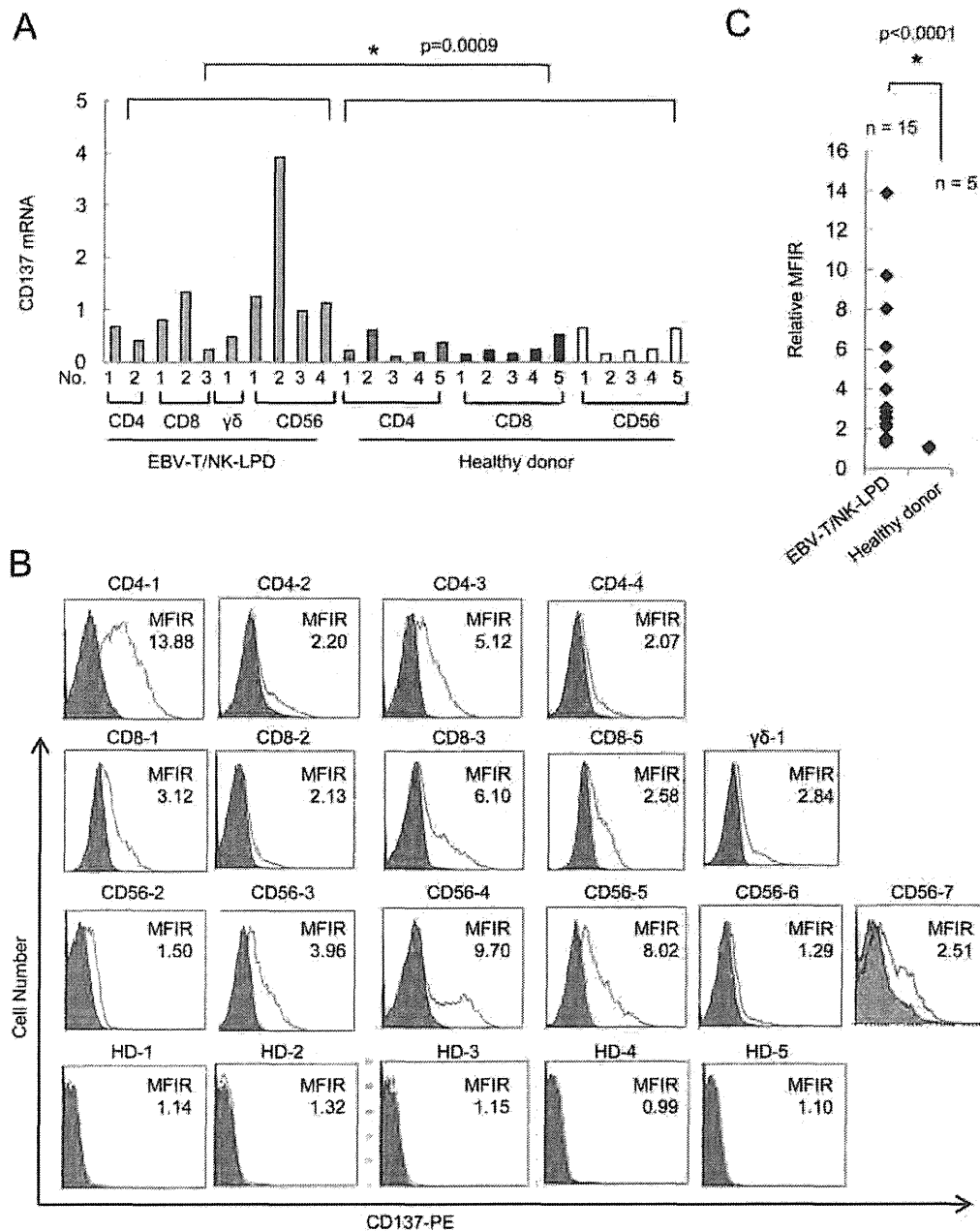doi:10.1371/journal.pone.0112564.t001

Figure 3. CD137 expression in EBV-positive T or NK cells of patients with EBV-T/NK-lymphoproliferative disorders (EBV-T/NK-LPDs). (A) Transcripts of *CD137* and *GAPDH* of freshly isolated EBV-positive cell fractions from 9 EBV-T/NK-LPDs patients, or cells of the same fractions from healthy donors were quantified by real-time RT-PCR. Relative copy number was obtained by normalizing the *CD137* transcripts to those of *GAPDH*. The relative copy number of the EBV-T/NK-LPDs patients' cells and healthy donor cells were compared. (B) CD137 protein expression in peripheral blood mononuclear cells (PBMCs) from 15 EBV-T/NK-LPDs patients or 5 healthy donors. PBMCs were cultured with IL-2 for 3 days and examined by flow cytometry. The mean fluorescent intensity of CD137 was normalized by that of isotype-matched control and expressed as MFIR (mean fluorescence intensity rate). (C) A bar graph for the relative MFIRs. Each point represents the MFIR of each sample.
doi:10.1371/journal.pone.0112564.g003

development of T or NK cell neoplasms have been reported to date. In this study we examined EBV-positive T or NK cells, and demonstrated that not only the cell lines but also freshly isolated cells of EBV-positive fractions from EBV-T/NK-LPDs patients expressed high levels of *CD137* mRNA. CD137 expression was also detected in EBV-positive cells isolated from the tissue lesions of EBV-T/NK-LPDs xenograft models. We demonstrated that EBV could directly induce CD137 expression most likely through LMP1 in T and NK cells. In addition, stimulation of CD137 by its

ligand could suppress etoposide-induced cell death in EBV-positive and CD137-expressing T or NK cells. These results suggested that EBV could promote survival of T and NK cells by inducing CD137 and might be a cause for EBV-T/NK-neoplasms.

In the present study, *CD137* gene expression was significantly higher in freshly isolated EBV-positive T or NK cells from PB of patients compared with lymphocytes from healthy donors. *In vitro* IL-2 treatment enhanced CD137 expression in the EBV-infected
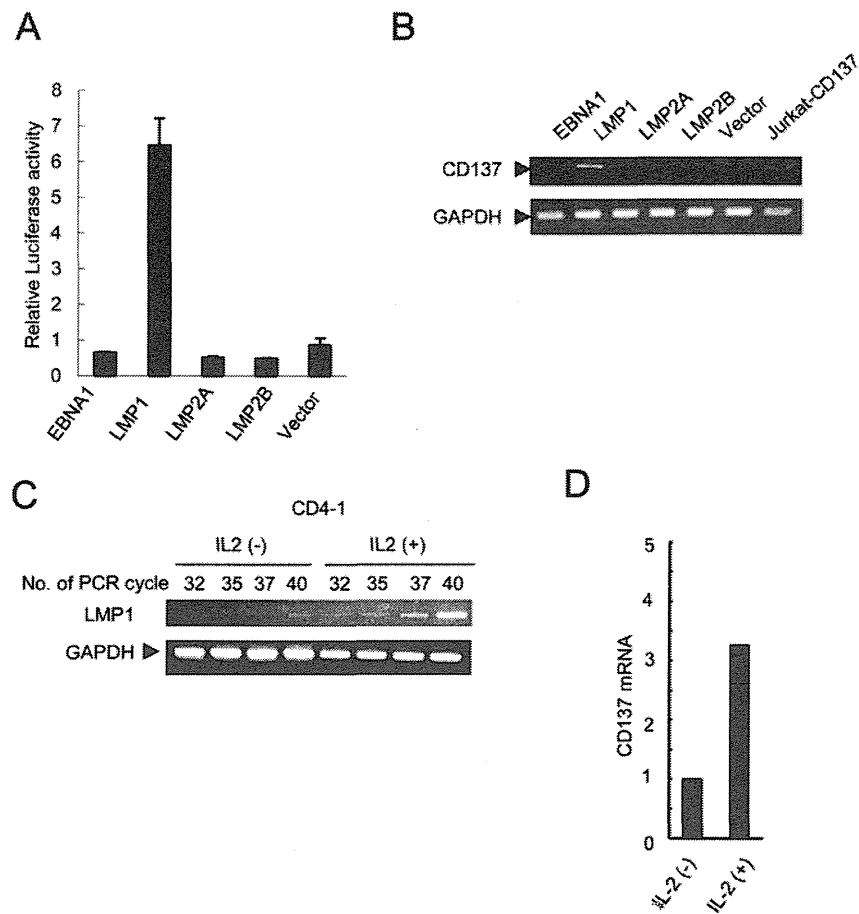
—114—

A

Relative Luciferase activity (y-axis: 0–8)

EBNA1, LMP1, LMP2A, LMP2B, Vector

B

EBNA1 LMP1 LMP2A LMP2B Vector Jurkat-CD137

CD137 ▶

GAPDH ▶

C

CD4-1

IL2 (-)   IL2 (+)

No. of PCR cycle   32 35 37 40   32 35 37 40

LMP1

GAPDH ▶

D

CD137 mRNA (y-axis: 0–5)

IL-2 (-)   IL-2 (+)

Figure 4. CD137 expression was upregulated by LMP1 whose expression was enhanced by IL-2 in EBV-T/NK-LPDs cells. (A) *CD137* transcription was examined using the assay described. Briefly, MOLT4 cells were transfected with 10 µg of the expression plasmids of the viral proteins, EBNA1, LMP1, LMP2A, LMP2B, or an empty vector as indicated, along with 10 µg of PGL3-4-1BB and 1 µg of pRLSV40. Twelve hours after transfection, the cells were harvested for a dual luciferase assay. Luciferase activity was normalized by *Renilla* luciferase activity and expressed in arbitrary units. The data are expressed as mean ± S.D. of 3 independent experiments. (B) MOLT4 cells were transfected with 10 µg of the expression plasmids of the viral proteins, EBNA1, LMP1, LMP2A, LMP2B, or an empty vector. Transcripts of CD137 (the upper panel) and GAPDH (the lower panel) in these cells were examined by RT-PCR. Jurkat-CD137 cells were used as a positive control. (C) RNAs were obtained from PBMCs from a EBV-T/NK-LPDs patient (CD4-1) which had been cultured with or without IL-2 for 3 days. Semi-quantitative RT-PCR assay for *LMP* was performed. Transcripts of *LMP1* (the upper panel) and *GAPDH* (the lower panel) were presented. (D) Transcripts of *CD137* and *GAPDH* were quantified by real time RT-PCR for the sample of 4C. Relative copy number was obtained by normalizing the *CD137* transcripts to those of *GAPDH*.
doi:10.1371/journal.pone.0112564.g004

Table 2. IL-2 concentration of the serum from EBV-T/NK-LPD patients.

EBV-T/NK-LPD (U/ml)		Healthy donor IL-2 (U/ml)
Case	IL-2 (U/ml)	
CD4-2	<0.8	<0.8
CD4-3	1.9	<0.8
CD4-5	0.9	<0.8
CD4-6	2.4	<0.8
CD8-2	2.1	1
CD8-3	1.1	
CD56-2	0.9	
CD56-3	0.9	

The concentration of IL-2 of the serum from EBV-T/NK-LPDs patients and from healthy donors. The lowest detection limit was 0.8 U/ml.
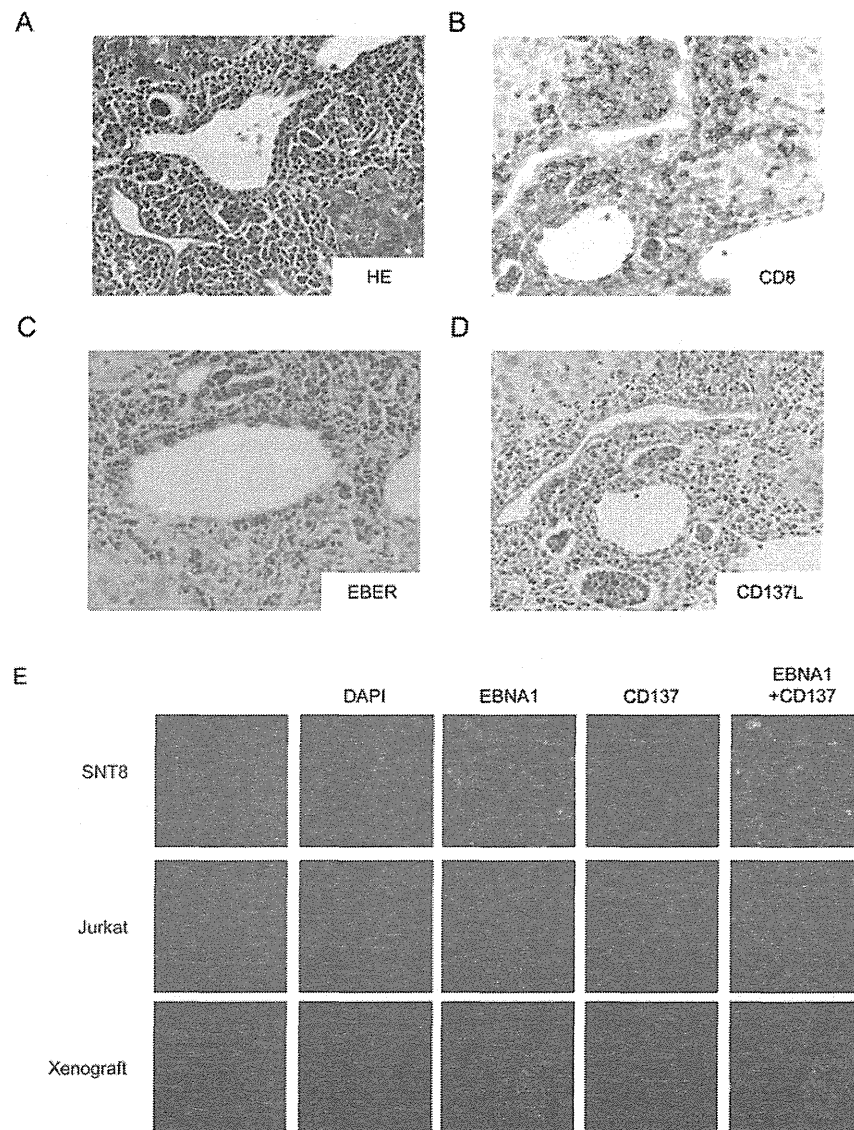doi:10.1371/journal.pone.0112564.t002

—115—

A

B

C

D

E

Figure 5. Histopathological specimen from the liver of the xenograft models. We generated the models by transplanting the cells from CD8-3 patient. Nine mice were examined and the representative data were shown. (A) Hematoxylin and eosin staining showed periportal infiltration of lymphocytes. (B) Immunochemical staining with anti-CD8 antibody (brown) showed that the infiltrating lymphocytes were positive for CD8. (C) In situ hybridization of Epstein–Barr virus-encoded mRNA (EBER) (brown). Infiltration of EBV-positive cells was detected in the periportal space. (D) Immunochemical staining with anti-CD137L antibody (brown) showed that CD137L-positive cells existed in the periportal space although the number of the cells was smaller than that of EBER positive cells. (original magnification, ×400). (E) Immune-fluorescent staining with anti-EBNA1 and anti-CD137 antibodies of cells isolated from the lesions. Mononuclear cells were obtained from the tissue lesions of a model mouse, stained with the antibodies. The cells were analyzed by confocal microscopy.
doi:10.1371/journal.pone.0112564.g005

cells of the patients, whereas not in control cells of the healthy donors. IL-2 treatment also increased *LMP1* gene expression in EBV-positive cells of EBV-T/NK-LPDs. Takahara and colleagues previously reported that IL-2 enhanced LMP1 expression in EBV-positive ENKL cell lines [18]. Since *CD137* promoter activity was enhanced by LMP1, we suggested that IL-2-induced CD137 protein expression was mediated by LMP1. In addition, the concentration of IL-2 in the serum of EBV-T/NK-LPDs patients was higher than that of healthy donors. Actually the concentration was lower than that of the culture medium, which we used in the assay. Ohga and colleagues, however, reported that the transcription of *IL-2* gene was upregulated in EBV-positive T- or NK-cells [19]. This finding suggested that the level might be high in the

tissue lesion where large amount of EBV-positive T- or NK-cell were infiltrating. We detected CD137 protein expression in EBV-positive cells isolated from the lesion. The high expression level of *CD137* mRNA in the circulating EBV-positive cells may contribute to rapid and strong induction of the protein expression in the lesions.

We suggested that EBV enhanced *CD137* mRNA expression through LMP1. Expression level of LMP1 in ENKL is actually variable and other factors, such as miRNA, may play roles for lymphomagenesis in EBV-positive T- or NK-neoplasms [20]. However, all EBV-positive T- or NK-cell lines examined in the present study, expressed LMP1 according to our results (data not shown) and the report [14]. LMP1 activates c-JUN N-terminal
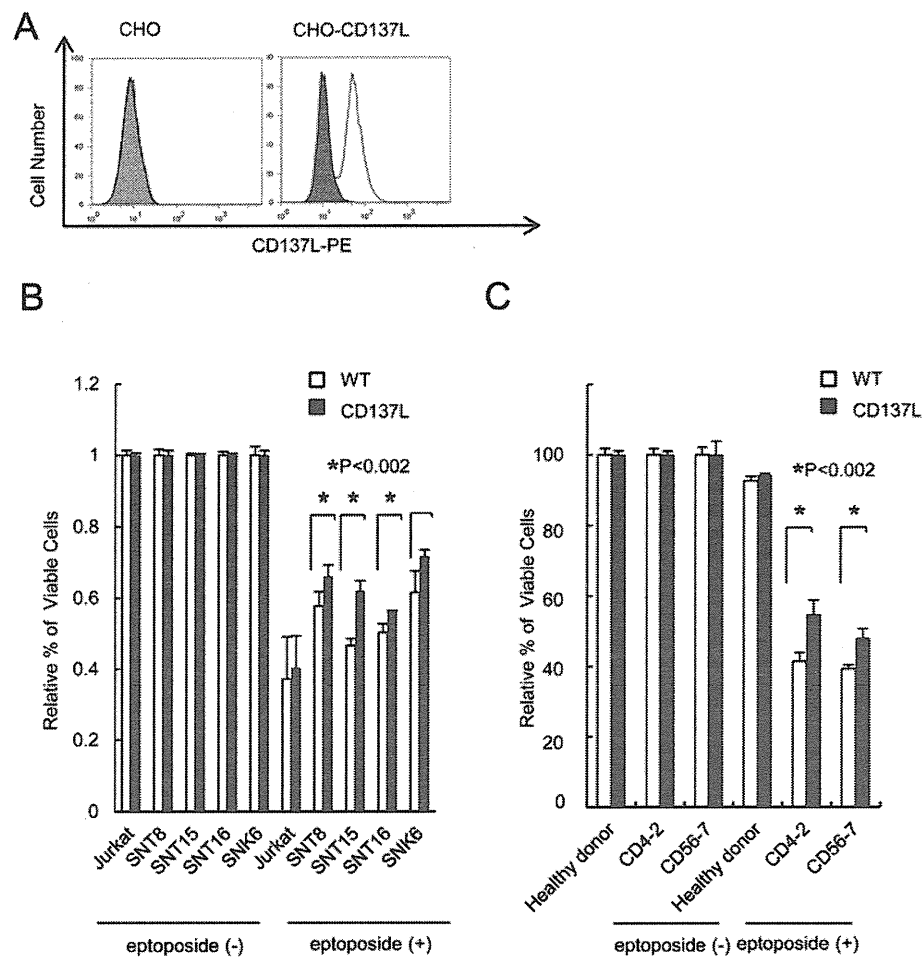
—116—

Figure 6. Stimulation of CD137 decreases etoposide-induced cell death of cells from patients with EBV-T/NK-LPDs. (A) CD137L expression on control Chinese Hamster Ovary (CHO) and CHO-CD137L cells. The expression was analyzed by flow cytometry using an antibody to CD137L (open histogram) or isotype-matched control immunoglobulin (gray, shaded histogram). (B) Jurkat cells and EBV- positive T- or NK-cell lines were cultured with 175 U/ml of IL-2 for 48 hours. Then they were cultured on control CHO or CHO-CD137L cells, which had been stained with PKH-26, with or without 2 µM of etoposide for 48 hours. They were then removed for assessment of viability. The cells were stained with DiOC6 and living EBV-T/NK-LPDs cells were detected as PKH-26-negative and DiOC6-positive cells by flow cytometry. The graph chart represents the relative numbers of living cells normalized by those of control cells which were cultured without etoposide. The data are expressed as mean ± S.D. of 3 independent experiments. (C) The PBMCs of EBV-T/NK-LPDs patients and healthy donors were cultured with 175 U/ml of IL-2 for 48 hours. Then they were cultured on control CHO or CHO-CD137L cells. They were then removed for assessment of viability as in B. The graph chart represents the relative numbers of living cells normalized by those of control cells which were cultured without etoposide. The data are expressed as mean ± S.D. of 3 independent experiments.
doi:10.1371/journal.pone.0112564.g006

kinase (JNK) [21], p38 mitogen-activated kinase (p38) [22], and Erk [23], which mediate the AP-1-activating pathway, and also activates NF-κB [24]. It was reported that CD137 expression was regulated by AP-1 and NF-κB in activated T cells [25]. LMP1 can, therefore, induce CD137 expression through AP-1 and NF-κB in T cells. In addition, we reported previously that EBV infection induced ectopic CD40 expression in T-cells [26,27]. CD40 is known to activate NF-κB, JNK, p38 and Erk [28,29]. Also, CD40-induced CD137 expression was recently reported [30]. These results indicate that EBV-induced CD137 expression can be mediated by LMP1, directly as well as through CD40.

Some questions, however, remain to be answered. The first concerns the localization of the CD137L. CD137L expression is induced in T cells when they are activated. [10] Its expression is also detected on various cancer cells [31]. Furthermore, expression of CD137 and CD137L is induced by the viral protein, Tax in ATLL cells and mediates autocrine survival signals, leading to

proliferation of the infected cells and tumor development [12]. We therefore investigated CD137L expression on EBV-T/NK-cells themselves. However, we could not detect CD137L expression clearly on the surface of EBV-T/NK-LPDs cells. CD137L expression is usually detected not only on the surface of activated B and T cells, but also on antigen-presenting cells (APCs) such as dendritic cells, monocytes, and macrophages [32,33]. EBV-negative cells, including histiocytes and macrophages are detected in EBV-T/NK-LPDs lesions surrounding EBV-infected cells [3]. These cells may express CD137L on their surface. Interestingly, CD137L-positive cells were certainly present in the lesions of EBV-T/NK-LPDs (Figure 5D). Since the number of CD137L-positive cells was markedly smaller than that of EBV-positive cells, they were considered to be different cell types. As we previously described, we generated the models by injection of the PBMCs from the patients [15]. Further investigations is required to determine the phenotype of the CD137L-positive cells in the

—117—

lesions and to clarify whether these cells have some effects on EBV-positive cells, thereby contributing to disease progression. In addition, soluble CD137L (sCD137L) needs to be investigated. sCD137L is produced by lymphocytes or monocytes, with studies showing that it is present in PB of healthy donors and its level is increased in that of patients with hematological malignancies [34] and autoimmune diseases [35]. sCD137L may also have a role in hematopoietic neoplasm development, with its serum levels potentially being a prognostic factor in acute myeloid leukemia and myelodysplastic syndrome [36].

The next question is the actual role of CD137 in the disorders. EBV-T/NK neoplasms are not only lymphoid malignancies, but also have aspects of severe inflammatory diseases accompanied by high fever, cytokinemia, hemophagocytic syndrome and so on [3,18,37-39]. As CD137 mediates survival, proliferation, and cytokine production of CD137-expressing T cells, it may cause inflammation associated with the disease. In addition, CD137 acts as a "ligand" for CD137L. CD137L stimulation by CD137 also mediates intracellular signaling in CD137L-expressing cells [40]. In monocytes expressing CD137L, stimulation of the molecule induces proliferation and differentiation into DCs [41,42]. In B cells expressing CD137L, the stimulation induces proliferation, differentiation and production of immunoglobulins [43,44]. EBV-T/NK-neoplasms are associated with local and systemic inflammation, cytokinemia, or polyclonal gammopathy [38,39]. CD137 may therefore contribute to disease development by inducing not only survival of the infected cells but also inflammation. Inhibition of CD137-mediating signals by targeting CD137 or CD137L should be conducted in order to clarify their roles.

It is well known that CD137 activates survival-promoting molecules including NF-kB in activated T cells [10]. However, the role of the CD137-CD137L interaction *in vivo* is still controversial. Recently, an agonistic CD137 antibody was created and used for xenograft models of human disease, cancer, or autoimmune diseases. In some mouse cancer models, agonistic CD137 antibody induces tumor suppression by upregulating the immune reaction of cytotoxic T-cells against tumor cells [45,46]. On the other hand, in disease models of hyperimmune reactions such as asthma, GVHD, and autoimmune disease, the same antibody had the effect of suppressing T cells [47]. These findings show that CD137 regulates T-cell reactions both positively and negatively, and that the mechanism of the action *in vivo* is extremely complicated. As mentioned previously, EBV-T/NK-LPDs have two aspects: suppressed immune-reaction against EBV-T/NK-cells and a hyper-immune reaction as an inflammatory disease. The conflicting roles of the CD137–CD137L axis may be compatible with these clinical findings of EBV-T/NK-LPDs.

Our results indicate that upregulation of CD137 expression through LMP1 by EBV promotes cell survival in T or NK cells. This effect may contribute to the development of EBV-T/NK-neoplasms and suggests an attractive therapeutic target for the diseases.

Materials and Methods

Cells and reagents

The EBV-positive T/NK-cell (EBV-T/NK cell) lines SNT8, SNT15, SNT16, SNK1, SNK6, and SNK10 were cultured in RPMI containing 10% FCS and 175 U/ml of human IL-2 [14]. The EBV-negative T- and NK-cell lines, Jurkat, MOLT4, HPB-ALL, and MTA were cultured in RPMI containing 10% fetal calf serum (10% FCS-RPMI), whereas the EBV-negative NK-cell line, KHYG1 was cultured in 10% FCS-RPMI containing 175 U/ml of human interleukin-2 (IL-2). The B- cell lines, BJAB, Ramos, Raji,

MD901 [48], HS-Sultan, and LCL were cultured in RPMI containing 10% FCS-RPMI. Jurkat, MOLT4, BJAB, Ramos, HS-Sultan and Raji cells were obtained from the American Type Culture Collection. LCL was established as previously described [26]. The expression of the viral proteins in LCL was demonstrated in Figure S4. MTA cells were obtained from Japanese Collection of Research Bioresources Cell Bank. Jurkat-CD137 and Chinese Hamster Ovary (CHO)-CD137L were generated as previously described [30]. Human recombinant IL-2 was purchased from R&D systems (Abington, UK) and etoposide from Wako (Osaka, Japan).

PCR assay for CD137

The sequences of the PCR primers used for detection of the CD137 gene were as follows: forward, 5′-GTGCCAGATTT-CATCATGGG-3′ (exon 2 of CD137) and reverse, 5′-CAA-CAGCCCTATTGACTTCC-3′ (exon 9 of CD137). The expression levels of the CD137 gene were determined by quantitative PCR, as described previously [13].

Diagnosis of EBV-T/NK-LPDs

EBV-T/NK-LPDs was diagnosed according to the following criteria: the presence of characteristic symptoms, an increase in EBV DNA load in peripheral blood (PB), and the detection of clonally proliferating EBV-positive T or NK cells [4,49].

Detection and isolation of EBV-positive cells in EBV-T/NK-LPDs patients

Detection and isolation of EBV-infected cells were performed as described previously [27]. Briefly, peripheral blood mononuclear cells (PBMCs) from EBV-T/NK-LPDs patients were isolated by density gradient centrifugation using Separate-L (Muto Pure Chemical, Tokyo, Japan) and sorted into CD19-, CD4-, CD8-, or CD56-positive fractions by antibody-conjugated magnetic beads (IMag Human CD19, 4, 8, and 56 Particles-DM; BD Biosciences, Sparks, MD, USA). The fraction which was negative for these markers was considered γδ T cell fraction. The EBV DNA load in each fraction was then measured by the real-time RT-PCR [50] on the basis of the TaqMan system (Applied Biosystems, Foster City, CA, USA). The fraction with the highest titer was assumed to be that with EBV-positive cells. In order to examine *CD137* mRNA expression in the infected cell, we isolated EBV-positive cells from PBMCs by magnetic beads conjugating antibodies for the surface markers of the infected cells.

Antibodies

Mouse antihuman CD137-PE, CD4-FITC, CD8-FITC, CD56-FITC and CD137L-PE as well as their control isotype antibodies were purchased from Becton, Dickinson and Company (Franklin Lakes, NJ, USA).

In vitro EBV infection assay

MOLT4 cells were infected with EBV as described previously [26]. Briefly, EBV was prepared from culture medium of B95-8 cells as described [51], and then concentrated (200-fold) in RPMI medium 1640 supplemented with 10% FCS. The virus suspension was filtered (0.45 μm) and the recipient cells (2×10^6 to 1×10^7) were incubated in 1 or 5 ml of the suspension for 1 h, and then rinsed twice with culture medium (10% RPMI). The efficiency of infection was >90% as judged by EBNA1 staining. For inactivation of the EBV genome, 1 ml of virus suspension in a 100-mm dish was irradiated with UV (254 nm) at 1 J μcm^2 using a FUNA-UV-LINKER FS-800 (Funakoshi, Tokyo). Infection was

—118—

verified by EBV DNA quantification, and immune fluorescence staining of EBNA1 staining of the cells as described using Polyclonal Rabbit Anti-Human C3c Complement/FITC antibody (Dako, Glostrup, Denmark) [52].

PCR assay for EBV proteins

RT-PCR for detection of mRNA for the viral proteins, *LMP1, LMP2A, LMP2B* and *EBNA1* was performed according to the previous report [15].

Plasmids

The reporter plasmid PGL3-4-1BB for the detection of *CD137* promoter activation was kindly provided by Dr. Pichler [12]. The reporter plasmid for detection of NF-κB activation, pNF-κB-Luc, was purchased from Stratagene (Santa Clara, CA, USA), and the control *Renilla* luciferase plasmid pRL-SV40 from Promega (Madison, WI, USA). Plasmids containing EBV-encoded proteins, LMP1, LMP2A, LMP2B and EBNA1 were generated from the EBV-infected cell line B95-8 [53].

Luciferase reporter assays

The assays of transiently transfected cells were performed as described previously [54].

Measurement of serum IL-2

The concentration of IL-2 in the serum was examined by SRL, Inc. (Tokyo, Japan) using enzyme-linked immunosorbent assay (ELISA). The lowest detection limit was 0.8 U/ml.

Generation of the xenograft model of EBV-T/NK-LPDs

Male NOD/Shi-scid/IL-2Rγnull (NOG) mice were obtained from the Central Institute for Experimental Animals (Kawasaki, Japan) and maintained under specific pathogen-free conditions. The model was generated by injection of PBMCs from patients to six weeks old mice through the tail vein as described previously [15]. Intravenous anesthesia by tribromoethanol was performed in order to minimize suffering. Engraftment was determined by detecting EBV DNA in the peripheral blood. After engraftment, mice were euthanized via CO_2 inhalation and applied for pathological and virological analyses.

Immunohistochemistry

The 4 μm thick paraffin-embedded formalin-fixed tissue sections were de-paraffinized, and heat-based antigen retrieval was performed in 0.1 M citrate buffer (pH 6.0). Endogeneous peroxidase activity was inhibited using hydrogen peroxide. The primary antibodies for CD137 (ab3169) and CD137L (ab64912) were purchased from Abcam (Cambridge, MA, USA). The detection system was the streptavidin-biotin-peroxidase complex technique (ABC kit; Vector Laboratories, Burlingame, CA, USA) with diaminobenzidine (DAB; Nichirei Bioscience, Tokyo, Japan) as the chromogen. *In situ* hybridization (ISH) of Epstein–Barr virus-encoded mRNA (EBER) was performed for detection of EBV in tissue sections by Epstein-Barr Virus (EBER) PNA Probe/ Fluorescein (DAKO, Carpinteria, CA, USA) and second antibody for Fluorescein (Dako, Glostrup, Denmark).

Immune-fluorescent staining

The expression of CD137 protein on EBV-infected cells was examined by immune-fluorescent staining. Cells were fixed on slides by immersing in 4% paraformaldehyde for 10 min, followed by washing three times in PBS and incubation with mouse monoclonal anti-CD137, goat polyclonal anti-EBNA1) antibodies

(Abcam, Cambridge, MA, USA), Cy5-conjugated Affinipure donkey anti-mouse antibody, and FITC-conjugated donkey anti-goat antibody (Jackson ImmunoResearch Laboratories, Inc. PA, USA). Nuclei were counterstained with ProLong Gold and DAPI (Invitrogen, Carlsbad, CA, USA), and the cells were analyzed by confocal microscopy (Fluoview FV10i, Olympus).

Stimulation of CD137 by ligand-expressing cells and detection of cell viability

The PBMCs were isolated from patients of EBV-T/NK-LPDs. Control CHO or CHO-CD137L cells were stained with PKH-26 (PKH-26 Red Fluorescent Cell Linker Kit; Sigma-Aldrich, St. Louis, MO, USA) according to the manufacturer's instructions, and plated on the wells. The PBMCs were then overlaid on pre-seeded control CHO or CHO-CD137L cells, and cultured with or without etoposide in 10% FCS-RPMI containing 175 U/ml of IL-2. After 48 h incubation, the cells were stained with DiOC6 (Invitrogen, Carlsbad, CA, USA) and removed. The cells were analyzed using a FACS Calibur flow cytometer (Becton, Dickinson and Company, Franklin Lakes, NJ USA), with PKH-26–negative and DiOC6-positive cells considered as living EBV-T/NK cells.

Statistical analysis

For statistical analyses of Figure 3A and 3B, Mann-Whitney test was performed using GraphPad Prism 5 (GraphPad Software, La Jolla, CA, USA). Student *t* test was performed for Figure 6B and 6C.

The study complied with the principles of the Declaration of Helsinki and was approved by the ethical committee of Tokyo Medical and Dental University (TMDU). Written informed consent was obtained from each patient. The experiments with NOG mice are in accordance with the Guidelines for Animal Experimentation of the Japanese Association for Laboratory Animal Science, as well as ARRIVE guidelines [55]. The experiments were approved by the Institutional Animal Care and Use Committee of TMDU (No. 0140087A).

Supporting Information

Figure S1 CD137L expression in EBV-positive cell lines. Surface expression of CD137L was examined by flow cytometry using an antibody to CD137L (open histogram) or isotype-matched control immunoglobulin (gray, shaded histogram). The mean fluorescent intensity of CD137 was normalized by that of isotype-matched control and expressed as MFIR (mean fluorescence intensity rate) in arbitrary units. CHO-CD137L cells were used as positive control.
(TIF)

Figure S2 CD137 expression in PBMCs from EBV-positive T-NK-lymphoproliferative patients and those from healthy donors (HD). After collection, the cells were cultured with IL-2 for 3 days. The expression was analyzed by flow cytometry using an antibody to CD137 and to surface protein expressed on EBV-positive cells.
(TIF)

Figure S3 Immune-fluorescent staining with anti-LMP1 antibody of cells isolated from the lesions. Mononuclear cells were obtained from the tissue lesions of a model mouse, stained with the antibody. The cells were analyzed by confocal microscopy.
(TIF)

Figure S4 LCL that we used in the study was established as previously described [26]. The infection was confirmed by

—119—

RT-PCR for EBNA. We also examined and detected the expression of the lytic protein, BZLF1 [56]. Akata cells [57] stimulated with IgG were used as a positive control for BZLF1 expression. Since BZLF1 was not expressed in them, we concluded that the infection was latent.
(TIF)

Acknowledgments

Author Contributions

Conceived and designed the experiments: MY KII SY SF OM AA. Performed the experiments: MY KII LW HK YS TF MK TK NS AA. Analyzed the data: MY KII LW HK YS TF MK TK NS SF OM AA. Contributed reagents/materials/analysis tools: MY KII YS SY TF TK SF OM AA. Wrote the paper: MY KII SY TK SF OM AA. Contributed to the modification of the draft and approved the final submission: MY KII HK LW YS SY TF MK TK NS SF OM AA.

References

1. Chan JKC, Quintanilla-Martinez L, Ferry JA, Peh S-C (2008) Extranodal NK/T-cell lymphoma, nasal type. In: Jaffe E, Harris N, Stein H, editors. World Health Organization Classification of Tumors Pathology and Genetics of Tumours of Haematopoietic and Lymphoid Tissues. Lyon IARC Press. pp. 285–289.

2. Chan JKC, Jaffe ES, Ralfkiaer E, Ko Y-H (2008) Aggressive NK-cell leukemia. In: ES J, NL H, H S, editors. World Health Organization Classification of Tumors Pathology and Genetics of Tumours of Haematopoietic and Lymphoid Tissues. Lyon: IARC Press. pp. 276–277.

3. Quintanilla-Martinez L, Kimura H, Jaffe ES (2008) EBV-positive T-cell lymphoproliferative disorders of childhood. In: Jaffe E, Harris N, Stein H, editors. World Health Organization Classification of Tumors Pathology and Genetics of Tumours of Haematopoietic and Lymphoid Tissues.Lyon IARC Press. pp. 278–280.

4. Kimura H, Ito Y, Kawabe S, Gotoh K, Takahashi Y, et al. (2012) EBV-associated T/NK-cell lymphoproliferative diseases in nonimmunocompromised hosts: prospective analysis of 108 cases. Blood 119: 673–686.

5. Kimura H, Hoshino Y, Kanegane H, Tsuge I, Okamura T, et al. (2001) Clinical and virologic characteristics of chronic active Epstein-Barr virus infection. Blood 98: 280–286.

6. Arai A, Imadome K, Watanabe Y, Yoshimori M, Koyama T, et al. (2011) Clinical features of adult-onset chronic active Epstein-Barr virus infection: a retrospective analysis. Int J Hematol 93: 602–609.

7. Kawa K, Sawada A, Sato M, Okamura T, Sakata N, et al. (2011) Excellent outcome of allogeneic hematopoietic SCT with reduced-intensity conditioning for the treatment of chronic active EBV infection. Bone Marrow Transplant 46: 77–83.

8. Yamaguchi M, Kwong YL, Kim WS, Maeda Y, Hashimoto C, et al. (2011) Phase II study of SMILE chemotherapy for newly diagnosed stage IV, relapsed, or refractory extranodal natural killer (NK)/T-cell lymphoma, nasal type: the NK-Cell Tumor Study Group study. J Clin Oncol 29: 4410–4416.

9. Yamaguchi M, Tobinai K, Oguchi M, Ishizuka N, Kobayashi Y, et al. (2012) Concurrent Chemoradiotherapy for Localized Nasal Natural Killer/T-Cell Lymphoma: An Updated Analysis of the Japan Clinical Oncology Group Study JCOG0211. J Clin Oncol.

10. Croft M (2009) The role of TNF superfamily members in T-cell function and diseases. Nat Rev Immunol 9: 271–285.

11. Pollok KE, Kim YJ, Zhou Z, Hurtado J, Kim KK, et al. (1993) Inducible T cell antigen 4-1BB. Analysis of expression and function. J Immunol 150: 771–781.

12. Pichler K, Kattan T, Gentzsch J, Kress AK, Taylor GP, et al. (2008) Strong induction of 4-1BB, a growth and survival promoting costimulatory receptor, in HTLV-1-infected cultured and patients' T cells by the viral Tax oncoprotein. Blood 111: 4741–4751.

13. Anderson MW, Zhao S, Freud AG, Czerwinski DK, Kohrt H, et al. (2012) CD137 is expressed in follicular dendritic cell tumors and in classical Hodgkin and T-cell lymphomas: diagnostic and therapeutic implications. Am J Pathol 181: 795–803.

14. Zhang Y, Nagata H, Ikeuchi T, Mukai H, Oyoshi MK, et al. (2003) Common cytological and cytogenetic features of Epstein-Barr virus (EBV)-positive natural killer (NK) cells and cell lines derived from patients with nasal T/NK-cell lymphomas, chronic active EBV infection and hydroa vacciniforme-like eruptions. Br J Haematol 121: 805–814.

15. Imadome K, Yajima M, Arai A, Nakazawa A, Kawano F, et al. (2011) Novel Mouse Xenograft Models Reveal a Critical Role of CD4 T Cells in the Proliferation of EBV-Infected T and NK Cells. PLoS Pathog 7: e1002326.

16. Tan JT, Ha J, Cho HR, Tucker-Burden C, Hendrix RC, et al. (2000) Analysis of expression and function of the costimulatory molecule 4-1BB in alloimmune responses. Transplantation 70: 175–183.

17. Lee HW, Park SJ, Choi BK, Kim HH, Nam KO, et al. (2002) 4-1BB promotes the survival of CD8+ T lymphocytes by increasing expression of Bcl-xL and Bfl-1. J Immunol 169: 4882–4888.

18. Takahara M, Kis LL, Nagy N, Liu A, Harabuchi Y, et al. (2006) Concomitant increase of LMP1 and CD25 (IL-2-receptor alpha) expression induced by IL-10 in the EBV-positive NK lines SNK6 and KAI3. Int J Cancer 119: 2775–2783.

19. Ohga S, Nomura A, Takada H, Ihara K, Kawakami K, et al. (2001) Epstein-Barr virus (EBV) load and cytokine gene expression in activated T cells of chronic active EBV infection. J Infect Dis 183: 1–7.

20. Yamanaka Y, Tagawa H, Takahashi N, Watanabe A, Guo YM, et al. (2009) Aberrant overexpression of microRNAs activate AKT signaling via down-regulation of tumor suppressors in natural killer-cell lymphoma/leukemia. Blood 114: 3265–3275.

21. Kutz H, Reisbach G, Schultheiss U, Kieser A (2008) The c-Jun N-terminal kinase pathway is critical for cell transformation by the latent membrane protein 1 of Epstein-Barr virus. Virology 371: 246–256.

22. Eliopoulos AG, Gallagher NJ, Blake SM, Dawson CW, Young LS (1999) Activation of the p38 mitogen-activated protein kinase pathway by Epstein-Barr virus-encoded latent membrane protein 1 coregulates interleukin-6 and interleukin-8 production. J Biol Chem 274: 16085–16096.

23. Dawson CW, Laverick L, Morris MA, Tramoutanis G, Young LS (2008) Epstein-Barr virus-encoded LMP1 regulates epithelial cell motility and invasion via the ERK-MAPK pathway. J Virol 82: 3654–3664.

24. Kaye KM, Izumi KM, Li H, Johannsen E, Davidson D, et al. (1999) An Epstein-Barr virus that expresses only the first 231 LMP1 amino acids efficiently initiates primary B-lymphocyte growth transformation. J Virol 73: 10525–10530.

25. Kim JO, Kim HW, Baek KM, Kang CY (2003) NF-kappaB and AP-1 regulate activation-dependent CD137 (4-1BB) expression in T cells. FEBS Lett 541: 163–170.

26. Imadome K, Shirakata M, Shimizu N, Nonoyama S, Yamanashi Y (2003) CD40 ligand is a critical effector of Epstein-Barr virus in host cell survival and transformation. Proc Natl Acad Sci U S A 100: 7836–7840.

27. Imadome K, Shimizu N, Arai A, Miura O, Watanabe K, et al. (2005) Coexpression of CD40 and CD40 ligand in Epstein-Barr virus-infected T and NK cells and their role in cell survival. J Infect Dis 192: 1340–1348.

28. Mukundan L, Bishop GA, Head KZ, Zhang L, Wahl LM, et al. (2005) TNF receptor-associated factor 6 is an essential mediator of CD40-activated proinflammatory pathways in monocytes and macrophages. J Immunol 174: 1081–1090.

29. Song Z, Jin R, Yu S, Rivet JJ, Smyth SS, et al. (2011) CD40 is essential in the upregulation of TRAF proteins and NF-kappaB-dependent proinflammatory gene expression after arterial injury. PLoS One 6: e23239.

30. Nakaima Y, Watanabe K, Koyama T, Miura O, Fukuda T (2013) CD137 Is Induced by the CD40 Signal on Chronic Lymphocytic Leukemia B Cells and Transduces the Survival Signal via NF-κB Activation. PLoS One 8: e64425.

31. Salih HR, Kosowski SG, Haluska VF, Starling GC, Loo DT, et al. (2000) Constitutive expression of functional 4-1BB (CD137) ligand on carcinoma cells. J Immunol 165: 2903–2910.

32. Alderson MR, Smith CA, Tough TW, Davis-Smith T, Armitage RJ, et al. (1994) Molecular and biological characterization of human 4-1BB and its ligand. Eur J Immunol 24: 2219–2227.

33. Pollok KE, Kim YJ, Hurtado J, Zhou Z, Kim KK, et al. (1994) 4-1BB T-cell antigen binds to mature B cells and macrophages, and costimulates anti-mu-primed splenic B cells. Eur J Immunol 24: 367–374.

34. Salih HR, Schmetzer HM, Burke C, Starling GC, Dunn R, et al. (2001) Soluble CD137 (4-1BB) ligand is released following leukocyte activation and is found in sera of patients with hematological malignancies. J Immunol 167: 4059–4066.

35. Jung HW, Choi SW, Choi JI, Kwon BS (2004) Serum concentrations of soluble 4-1BB and 4-1BB ligand correlated with the disease severity in rheumatoid arthritis. Exp Mol Med 36: 13–22.

36. Hentschel N, Krusch M, Kiener PA, Kolb HJ, Salih HR, et al. (2006) Serum levels of sCD137 (4-1BB) ligand are prognostic factors for progression in acute myeloid leukemia but not in non-Hodgkin's lymphoma. Eur J Haematol 77: 91–101.

37. Kimura H (2006) Pathogenesis of chronic active Epstein-Barr virus infection: is this an infectious disease, lymphoproliferative disorder, or immunodeficiency? Rev Med Virol 16: 251–261.

38. Kasahara Y, Yachie A, Takei K, Kanegane C, Okada K, et al. (2001) Differential cellular targets of Epstein-Barr virus (EBV) infection between acute EBV-associated hemophagocytic lymphohistiocytosis and chronic active EBV infection. Blood 98: 1882–1888.

—120—

39. Fox CP, Shannon-Lowe C, Gothard P, Kishore B, Neilson J, et al. (2010) Epstein-Barr virus-associated hemophagocytic lymphohistiocytosis in adults characterized by high viral genome load within circulating natural killer cells. Clin Infect Dis 51: 66–69.

40. Shao Z, Schwarz H (2011) CD137 ligand, a member of the tumor necrosis factor family, regulates immune responses via reverse signal transduction. J Leukoc Biol 89: 21–29.

41. Lee SW, Park Y, So T, Kwon BS, Cheroutre H, et al. (2008) Identification of regulatory functions for 4-1BB and 4-1BBL in myelopoiesis and the development of dendritic cells. Nat Immunol 9: 917–926.

42. Laderach D, Wesa A, Galy A (2003) 4-1BB-ligand is regulated on human dendritic cells and induces the production of IL-12. Cell Immunol 226: 37–44.

43. Pauly S, Broll K, Wittmann M, Giegerich G, Schwarz H (2002) CD137 is expressed by follicular dendritic cells and costimulates B lymphocyte activation in germinal centers. J Leukoc Biol 72: 35–42.

44. Middendorp S, Xiao Y, Song JY, Peperzak V, Krijger PH, et al. (2009) Mice deficient for CD137 ligand are predisposed to develop germinal center-derived B-cell lymphoma. Blood 114: 2280–2289.

45. Melero I, Shuford WW, Newby SA, Aruffo A, Ledbetter JA, et al. (1997) Monoclonal antibodies against the 4-1BB T-cell activation molecule eradicate established tumors. Nat Med 3: 682–685.

46. Narazaki H, Zhu Y, Luo L, Zhu G, Chen L (2010) CD137 agonist antibody prevents cancer recurrence: contribution of CD137 on both hematopoietic and nonhematopoietic cells. Blood 115: 1941–1948.

47. Seo SK, Choi JH, Kim YH, Kang WJ, Park HY, et al. (2004) 4-1BB-mediated immunotherapy of rheumatoid arthritis. Nat Med 10: 1088–1094.

48. Miki T, Kawamata N, Arai A, Ohashi K, Nakamura Y, et al. (1994) Molecular cloning of the breakpoint for 3q27 translocation in B-cell lymphomas and leukemias. Blood 83: 217–222.

49. Okano M, Kawa K, Kimura H, Yachie A, Wakiguchi H, et al. (2005) Proposed guidelines for diagnosing chronic active Epstein-Barr virus infection. Am J Hematol 80: 64–69.

50. Kimura H, Morita M, Yabuta Y, Kuzushima K, Kato K, et al. (1999) Quantitative analysis of Epstein-Barr virus load by using a real-time PCR assay. J Clin Microbiol 37: 132–136.

51. Sinclair AJ, Palmero I, Peters G, Farrell PJ (1994) EBNA-2 and EBNA-LP cooperate to cause G0 to G1 transition during immortalization of resting human B lymphocytes by Epstein-Barr virus. EMBO J 13: 3321–3328.

52. Reedman BM, Klein G (1973) Cellular localization of an Epstein-Barr virus (EBV)-associated complement-fixing antigen in producer and non-producer lymphoblastoid cell lines. Int J Cancer 11: 499–520.

53. Shirakata M, Imadome KI, Okazaki K, Hirai K (2001) Activation of TRAF5 and TRAF6 signal cascades negatively regulates the latent replication origin of Epstein-Barr virus through p38 mitogen-activated protein kinase. J Virol 75: 5059–5068.

54. Nosaka Y, Arai A, Miyasaka N, Miura O (1999) CrkL mediates Ras-dependent activation of the Raf/ERK pathway through the guanine nucleotide exchange factor C3G in hematopoietic cells stimulated with erythropoietin or interleukin-3. J Biol Chem 274: 30154–30162.

55. MacCallum CJ (2010) Reporting animal studies: good science and a duty of care. PLoS Biol 8: e1000413.

56. Iwasaki Y, Chong JM, Hayashi Y, Ikeno R, Arai K, et al. (1998) Establishment and characterization of a human Epstein-Barr virus-associated gastric carcinoma in SCID mice. J Virol 72: 8321–8326.

57. Takada K, Horinouchi K, Ono Y, Aya T, Osato T, et al. (1991) An Epstein-Barr virus-producer line Akata: establishment of the cell line and analysis of viral DNA. Virus Genes 5: 147–156.

—121—

Survival rates and prognostic factors of Epstein–Barr virus-associated hydroa vacciniforme and hypersensitivity to mosquito bites

T. Miyake,[1] T. Yamamoto,[1,2] Y. Hirai,[1] M. Otsuka,[1] T. Hamada,[1] K. Tsuji,[1] S. Morizane,[1] D. Suzuki,[1] Y. Aoyama[1] and K. Iwatsuki[1]

[1]Department of Dermatology, Okayama University Graduate School of Medicine, Dentistry and Pharmaceutical Sciences, 2-5-1 Shikata-cho Kita-ku, Okayama 700-8558, Japan
[2]Department of Dermatology, Kawasaki Medical School, Okayama, Japan

Summary

Background Epstein-Barr virus (EBV)-associated T/natural-killer lymphoproliferative disorders form a group of diseases that includes classical and systemic hydroa vacciniforme (HV) and hypersensitivity to mosquito bites (HMB). Patients with systemic HV (sHV) and HMB often have a poor prognosis, although little is known about the prognostic factors.

Objectives To elucidate the prognostic factors of HV and HMB.

Methods We studied clinicopathological manifestations, routine laboratory findings, anti-EBV titres, EBV DNA load and EBV-encoded gene expression, including expression of BZLF1, in 50 patients with classical HV (cHV), sHV, HMB only and HMB with HV (HMB + HV), and further analysed 30 patients who were available for follow-up.

Results The median age of disease onset was 5 years (range 1–74). A follow-up study indicated that fatal outcomes were observed in three of eight patients with sHV, two of six patients with HMB only, and two of five patients with HMB + HV. The main causes of death were complications from haematopoietic stem-cell transplantation and multiorgan failure. There were no fatalities among the 11 patients with cHV. Univariate analysis revealed two poor prognostic indicators: (i) onset age > 9 years and (ii) the expression of an EBV-encoded immediate–early gene transcript, BZLF1 mRNA, in the skin lesions (P < 0·001 and P = 0·003, respectively).

Conclusions No prognostic correlation was observed in EBV-infected lymphocyte subsets, anti-EBV antibody titres or EBV DNA load. Late onset and EBV reactivation are both related to more severe phenotypes of the disease, and thus may predict a poor prognosis.

What's already known about this topic?

- Epstein–Barr virus-associated T/natural-killer lymphoproliferative disorders form a group of diseases that includes classical and systemic hydroa vacciniforme (HV), and hypersensitivity to mosquito bites (HMB).
- Patients with systemic HV and HMB usually present with fever, liver damage and haematological abnormalities, and often have a fatal outcome.

What does this study add?

- Our patients with classical HV showed a favourable prognosis, while approximately one-third of the patients with systemic HV or HMB died during the 10-year follow-up.
- Late onset (over 9 years of age) and an EBV reactivation signal (BZLF1 mRNA expression) were both related to more severe phenotypes of the disease, and a poor prognosis.

Epstein-Barr virus (EBV)-associated T/natural-killer (NK) lymphoproliferative disorders (LPDs) form a group of diseases including hydroa vacciniforme (HV) and hypersensitivity to mosquito bites (HMB). EBV-associated HV lesions contain a number of EBV-encoded small nuclear RNA (EBER)[+] T cells, together with larger numbers of EBER[−] cytotoxic T lymphocytes (CTLs). Meanwhile, NK cells are absent or occur at background levels in such lesions.[1,2] Although there are no systemic symptoms or abnormalities in the routine laboratory tests of patients with classical HV (cHV), EBV DNA load and EBV^{+} γδT cells are increased in the peripheral blood mononuclear cells (PBMCs).[3] In contrast, patients with HV-like ulcerative cutaneous eruptions often present with systemic symptoms such as fever, hepatic damage and lymphadenopathy (systemic HV, sHV), and show dense inflammatory-cell infiltrates that reach the subcutaneous tissue. As reported previously, patients with cHV may progress to sHV in the clinical course.[2]

HMB is an EBV-associated T/NK LPD characterized by intense local skin reactions and systemic symptoms, including high fever, lymphadenopathy, hepatosplenomegaly and haemophagocytic syndrome.[4] These clinical symptoms can be induced by mosquito bites, other insect bites or vaccination. Patients with HMB usually have EBV[+] NK-cell lymphocytosis,[3,5] and HV-like eruptions may occur over the course of the disease. We previously examined differences in cellular events between HMB and HV-like eruptions.[3] Our results indicated that many CD56^{+} NK cells and T cells are present in the subcutaneous infiltrates in HMB, but no CD56^{+} NK cells occur in HV dermal infiltrates.

Unlike cHV, both sHV and HMB have been reported in Asian and Latin American countries.[6–8] However, the nomenclature of EBV-associated T/NK LPDs has been controversial. Patients with sHV in the present study may be synonymous with HV-like lymphoma in the World Health Organization classification,[9] and may overlap with chronic active EBV infection (CAEBV) and EBV-associated haemophagocytic lymphohistiocytosis (HLH).[10] Because of the diagnostic value of HV-like cutaneous signs, we have used the terms HV and HMB in our classification, excluding the diagnoses of CAEBV and HLH.

Although no prognostic markers have been elucidated, previous reports of CAEBV indicate that patients with the EBV[+] T-cell-predominant type have a poorer prognosis than those with the EBV[+] NK-cell-predominant type, and that late onset may be a risk factor.[10] In the present study, we attempted to clarify cellular and molecular markers related to the prognosis of cutaneous EBV-associated T/NK LPDs in a series of patients with HV and HMB, and to verify the validity of diagnostic criteria to distinguish benign from malignant types for the purposes of prognosis.

Patients and methods

Patients

Fifty patients were categorized into four groups: cHV (23 cases), sHV (12 cases), HMB only (nine cases) and

HMB + HV (six cases), according to the criteria in Table 1. Briefly, patients with cHV presented with lesions defined as vesiculopapules on sun-exposed areas without any systemic symptoms or abnormalities in routine laboratory test results. Patients with sHV presented with HV-like eruptions associated with systemic symptoms such as fever and lymphadenopathy and/or abnormalities in routine blood examinations at diagnosis. In our series, one of 12 patients with sHV initially had skin symptoms without systemic symptoms, although the patient had an increased percentage of NK cells (> 30% of lymphocytes) in the blood test. HMB is defined as an intense skin response to mosquito bites, insect bites or vaccination associated with systemic symptoms and/or abnormalities in routine blood tests.

Skin biopsy materials, crusts and blood samples were obtained for diagnosis, and used for in situ hybridization with EBER and quantitative reverse-transcriptase polymerase reaction (RT-PCR) to detect EBV infection in skin lesions.

This study was approved by the ethical committee (the institutional review board of Okayama University Hospital, no. 419, 2011) in accordance with the 1975 Declaration of Helsinki.

Assay for Epstein–Barr virus DNA load in peripheral blood mononuclear cells

DNA was extracted from 1×10^6 PBMCs using a QIAamp[™] Blood Kit (Qiagen, Venlo, the Netherlands), and the PCR amplification was performed using QuantiTect[™] Probe PCR (Qiagen) with Roche Light cycler (Roche, Pleasanton, CA, U.S.A.). The PCR primers for this assay were selected in the BamHI M region (BMRF1). The upstream and downstream primer sequences were 5′-GTGCCAATCTTGAGGTTTTAC-3′ and 5′-CACCCGGGGACTTTTATC-3′, respectively. The fluorogenic probes used were probe A, 5′-GACCTGCCGTTGGATCTTA GTG-3′, and probe B, 5′-TATTTTATTTAACCACGCCTCCGA AGA-3′. Amplification was carried out at 95 °C for 15 min, followed by 50 cycles of 95 °C for 15 s, 56 °C for 20 s and 72 °C for 15 s. The semiquantitative amounts of EBV DNA copies in patients' samples were determined from the standard curve obtained by PCR amplification of serial 10-fold dilutions of the template plasmid DNA solution.

Primer sets for reverse-transcriptase polymerase chain reaction

RNA was extracted from the samples with TRIzol[™] reagent (Gibco-BRL, Gaithersburg, MD, U.S.A.), and the cDNA was amplified by PCR using EBER1-specific and BamHI A rightward transcripts (BARTs)-specific primers, as described previously.[11,12] The integrity of the RNA was checked by the parallel amplification of beta-2-microglobulin (β2-MG). To detect EBV reactivation, BZLF1 was amplified by RT-PCR, using BZLF1-specific outer primers: sense, 5′-CATGTTTCAACCGC TCCGACTGG-3′, and antisense, 5′-GCGCAGCCTGTCATTTTCA GATG-3′. Amplification consisted of 40 cycles of 94 °C for

Table 1 Criteria for classical and systemic hydroa vacciniforme (HV) and hypersensitivity to mosquito bites (HMB)

	Classical HV	Systemic HV	HMB
Cutaneous lesion	Vesiculopapular lesion	Ulceronecrotic lesion	Swollen erythema or skin ulcer following mosquito bites, insect bites or vaccination
EBER-positive cells	+	+	+
Systemic symptoms and/or abnormality in routine laboratory findings[a]	−	+	+

EBER, Epstein–Barr virus-encoded small nuclear RNA. [a]Systemic symptoms include high-grade fever, lymphadenopathy and hepatosplenomegaly. Laboratory abnormalities include hepatic damage, haematological findings suggestive of haemophagocytic syndrome and natural-killer-cell lymphocytosis (> 30% of cells).

45 s, 64 °C for 30 s and 72 °C for 1 min. BZLF1-specific inner primers were sense, 5′-TCCCAGTCTCCGACATAACCCA-3′, and antisense, 5′-AGCAGCGACCTCACGGTAGT-3′; amplification involved 28 cycles of 94 °C for 45 s, 58 °C for 30 s and 72 °C for 1 min. Amplification gave 167 b.p. for EBER1 cDNA, 142 b.p. for BARTs cDNA, 295 b.p. for β2-MG cDNA and 332 b.p. for BZLF1 cDNA (639 b.p. for BZLF1 DNA).

Labelling for Epstein–Barr virus-encoded small nuclear RNA *in situ* hybridization

Lymphoid cells containing EBER1 were detected by *in situ* hybridization on paraffin-embedded sections, as described previously.[13] The density of EBER-positive cells was classified into four subgroups according to the percentage of positive cells: 1 + (1–5% positivity in the infiltrate); 2 + (5–25%); 3 + (25–50%) and 4 + (≥ 50%).

Immunophenotyping of infiltrating cells

Deparaffinized biopsy specimens were incubated with monoclonal antibodies to CD3ε, CD4, CD8, CD20, CD30 (Dako, Glostrup, Denmark) and CD56 (Novocastra Laboratories Ltd., Newcastle upon Tyne, U.K.), as described previously.[14]

Flow cytometric analysis for lymphocyte subsets

Blood samples from the patients were reacted with fluorescence-conjugated antibodies to CD3, CD56, T-cell receptor (TCR)αβ and TCRγδ (Beckman Coulter, Brea, CA, U.S.A.), and analysed using a FACSCalibur flow cytometer and CELL-QUEST software, version 5.2.1 (Becton Dickinson Co., Franklin Lakes, NJ, U.S.A.).

Statistical analysis

Analyses were performed using SPSS for Windows version 20.0 (IBM, Armonk, NY, U.S.A.). For univariate analyses, a one-sided Fisher's exact test was used to compare the categorical variable. To compare the quantitative variable, the Mann–Whitney U-test was used. For survival analysis, the

Kaplan–Meier method and log-rank test were used. In all analyses, P < 0·05 was considered significant.

Results

Clinical observations of the patients

Fifty patients (26 male and 24 female) were enrolled in the current study. They were classified into four groups: cHV, sHV, HMB only or HMB + HV, according to our tentative diagnostic criteria as described elsewhere (Table 1).[3] The age of onset ranged from 1 to 74 years (median 5 years). The median onset ages and the sexes of the four groups were as follows: cHV, 5 years (13 male, 10 female); sHV, 8 years (five male, seven female); HMB only, 8 years (six male, three female) and HMB + HV, 3·5 years (two male, four female). Of 23 patients with cHV, 21 (91%) had cutaneous lesions that presented within their first decade. The cutaneous signs of cHV occurred at younger ages than those of sHV and HMB + HV (P = 0·022 and P = 0·026, respectively).

Mucocutaneous symptoms such as conjunctivitis and oral aphthous stomatitis/gingivitis were observed in six (26%) of 23 patients with cHV and five (42%) of 12 patients with sHV, but were not observed in any of the nine patients with HMB or the six with HMB + HV. Of the 27 patients with sHV, HMB only or HMB + HV, 22 presented with systemic symptoms, including fever (22, 81%), diarrhoea (two, 7%), intestinal perforation (one, 4%), hepatosplenomegaly (11, 41%), myocarditis (two, 7%) and haemophagocytic syndrome (two, 7%) (Table 2).

Follow-up study

Of the 50 patients enrolled in the present study, 30 were included in a follow-up study; the time to follow-up ranged from 1 to 26 years (median 6·5 years). The median follow-up times for the four groups were 8 years for cHV, 7 years for sHV, 3 years for HMB only and 12 years for HMB + HV. All 11 patients with cHV were alive at follow-up, with or without disease, and nine of the 11 patients had been treated only with sunscreen. One of the two remaining patients, a